Clearance of persistent hepatitis C virus infection using a claudin-1-targeting monoclonal antibody

Laurent Mailly, Fei Xiao*, Joachim Lupberger*, Garrick K. Wilson, Philippe Aubert, François H. T. Duong, Diego Calabrese, Céline Leboeuf, Isabel Fofana, Christine Thumann, Simonetta Bandiera, Marc Lütgehetmann, Tassilo Volz, Christopher Davis, Helen J. Harris, Christopher J. Mee, Erika Girardi, Béatrice Chane-Woon-Ming, Maria Ericsson, Nicola Fletcher, Ralf Bartenschlager, Patrick Pessaux, Koen Vercauteren, Philip Meuleman, Pascal Villa, Lars Kaderali, Sébastien Pfeffer, Markus H. Heim, Michel Neunlist, Mirjam B. Zeisel, Maura Dandri, Jane A. McKeating, Eric Robinet[§] and Thomas F. Baumert[§]

*These authors contributed equally to the work.

[§]These authors contributed equally to the work.

Supplementary Information

SUPPLEMENTARY FIGURES

Supplementary Figure 1. Staining of CLDN1 in human chimeric-liver mice.

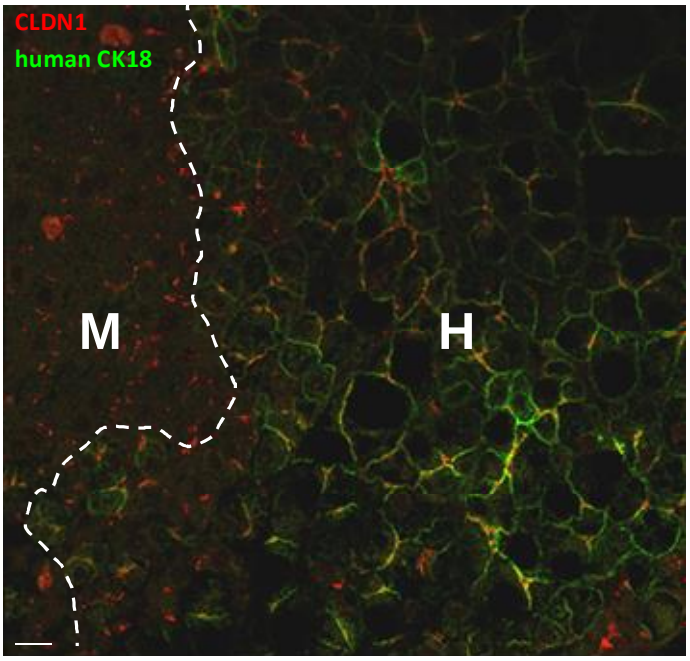

CLDN1 and human cytokeratin 18 (hCK18) expression in chimeric livers of uPA-SCID mice were assessed by confocal microscopy as described in Methods. Fluorescent images show CLDN1 (red) and hCK18 (green). CLDN1 staining appears in mouse (M) and human (H) areas confirming cross-reactivity of the antibody. Scale bars ï 20 µm.

Supplementary Figure 2. Tight junction ultrastructure in the liver of human chimeric mice.

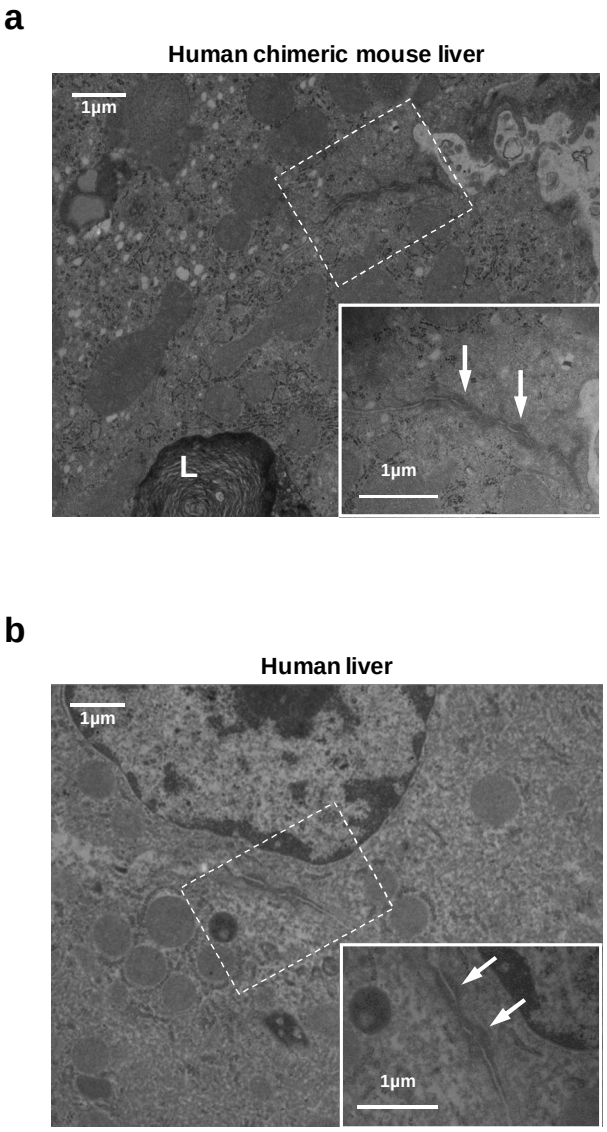

(**a, b**) Transmission electron microscopy analyses of tissue sections of chimeric human mouse liver from CLDN1-specific mAb-treated uPA-SCID mice (**a**) and human liver (**b**). The presence of Lipofuscin (L) which has been described to be a hallmark of human hepatocytes[1,2] suggests that the depicted hepatocyte is of human origin. White arrows indicate tight junctions which are indistinguishable in mice treated with CLDN1-specific antibody or human hepatocytes of human liver.

Supplementary Figure 3. Absence of antiviral resistance in mice treated with CLDN1-specific antibody.

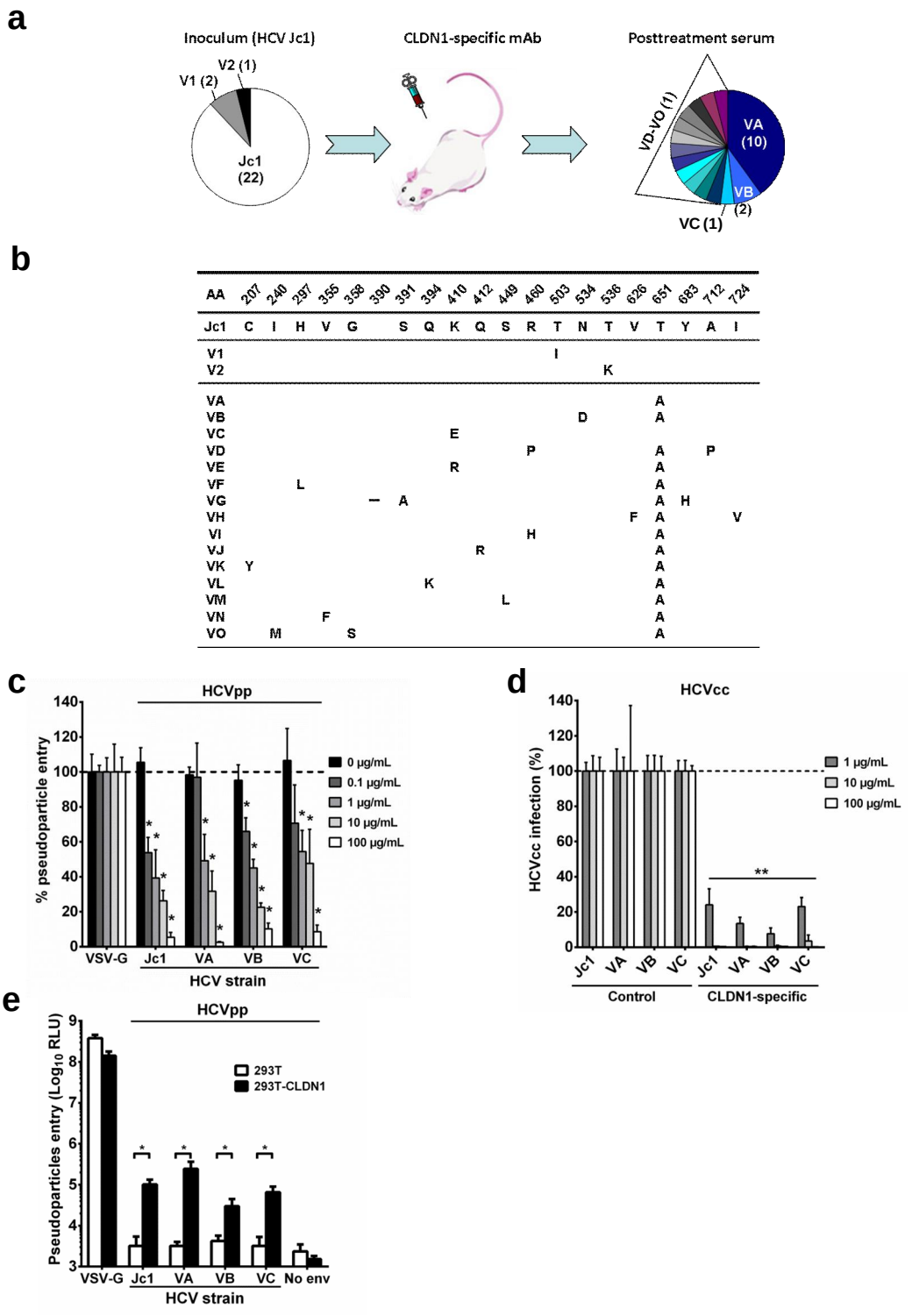

(**a**) Evolution of viral variants. HCV RNA was isolated and amplified from pre- and post-treatment serum of a chimeric mouse showing a viral relapse (Fig. 2c). Following cloning and sequencing of the entire E1E2 envelope glycoprotein coding region, the relative distribution of viral variants (VA to VO) was analyzed and is indicated in different colors. For each variant, the number of detected clones is indicated. (**b**) Comparative analysis of amino acid changes in the viral envelope

primary sequence in pre- and post-treatment samples. Differences compared to wild-type Jc1 are indicated. Amino acid deletion is denoted by ñ-ñ (**c**) Inhibition of HCVpp entry expressing mouse serum-derived viral envelopes by CLDN1-specific mAb. Huh7.5.1 cells were infected with HCVpp expressing envelopes of wild-type Jc1, VA, VB or VC variants (depicted in **b**) in the presence of increasing amount of CLDN1-specific mAb. Data are expressed as percent entry as compared to entry in the presence of control mAb (100%, dashed line). Means ± s.e.m. of three independent experiments performed in triplicate are shown. (**d**) Inhibition of HCVcc infection expressing mouse serum-derived viral envelopes by CLDN1-specific mAb. Huh7.5 cells were infected with HCVcc-Luc expressing envelopes of wild-type Jc1, VA, VB or VC variants (depicted in **b**) in the presence of increasing amount of CLDN1-specific mAb. HCVcc infection was assessed by determination of luciferase reporter activity. Data are expressed as percentage of infection as compared to infection in presence of control mAb (100%, dashed line). Means ± s.d of two independent experiments performed in duplicate are shown. Stars indicate significance as compared to each corresponding control. (**e**) HCVpp entry expressing mouse serum-derived viral envelopes is dependent on CLDN1 expression. 293T (white bars) or 293T expressing CLDN1 (black bars) were infected with HCVpp depicted in (**c**). Means ± s.d. of three independent experiments performed in triplicate are shown. Pseudoparticles expressing the VSV-G protein (VSV-Gpp) were used as control. VA, VB were chosen since they were the most frequent variants. VC was chosen since it was the only variant without mutation of residue 651. * $p < 0.01$, ** $p < 0.001$ (Student's t-test).

Supplementary Figure 4. Cell surface expression of CLDN1, 6 and 9 on engrafted primary human hepatocytes and Huh7.5.1 cells.

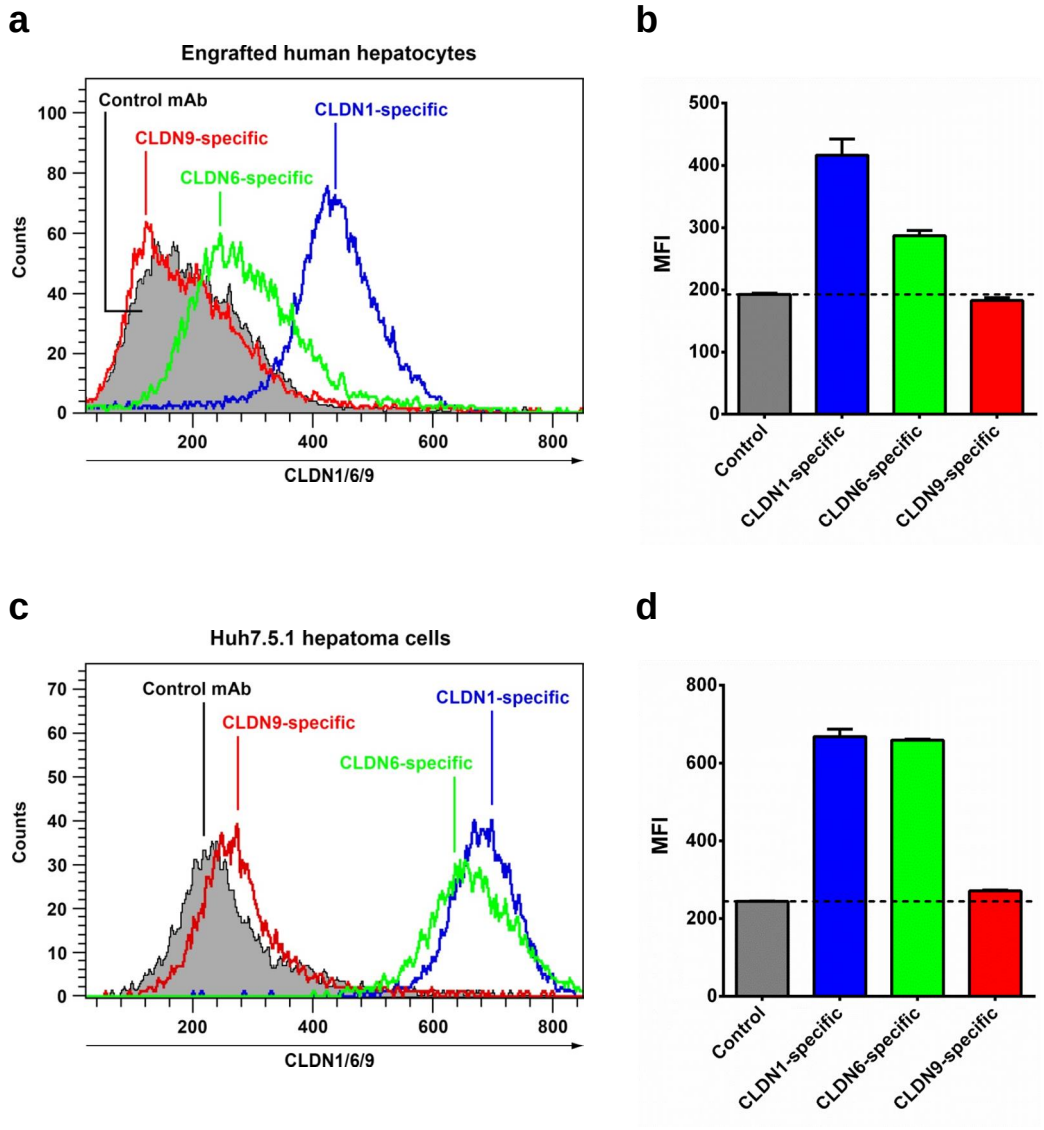

(**a, b**) Primary human hepatocytes used for engraftment of upA-SCID mice and (**c, d**) Huh7.5.1 cells were incubated with human CLDN1-, 6- and 9-specific rat mAbs (20 µg/mL) and expression of CLDNs was quantified by flow cytometry as described[3]. The mean fluorescence intensity (MFI) ± s.d. from two experiments performed in duplicate is shown in (**b, d**).

Supplementary Figure 5. Treatment of genotype 4 infected mice.

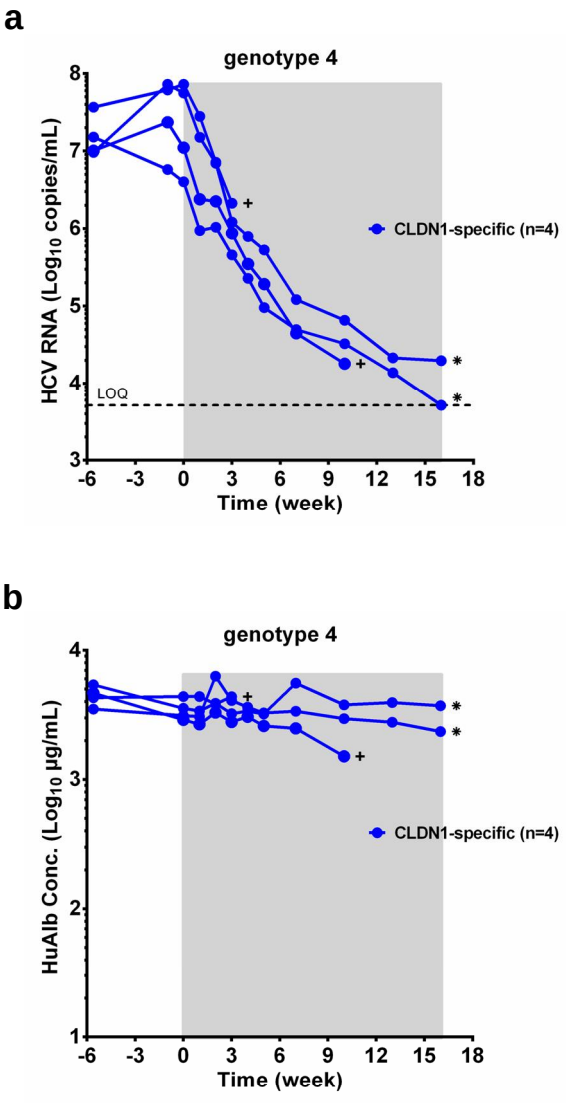

(**a**) Chimeric uPA-SCID mice were chronically infected with a genotype 4 (gt4) HCV-containing serum (ED43) described in prevention experiments (Fig. 2). Forty-two days following inoculation, the animals received 500 µg of CLDN1-specific mAb twice a week for 3 weeks, followed by 200 µg twice a week up to the end of the study period (grey box). Serum viral load was determined as described in Methods. (**b**) Serum human albumin from (**a**) was determined by a specific ELISA as described in Methods. A control mAb had no effect on viral infection with genotype 4 (Fig. 2b). Dead mice (cross) and mice sacrificed following ethical policy (star) are indicated.

Supplementary Figure 6. Safety of the CLDN1-specific mAb in chimeric mice.

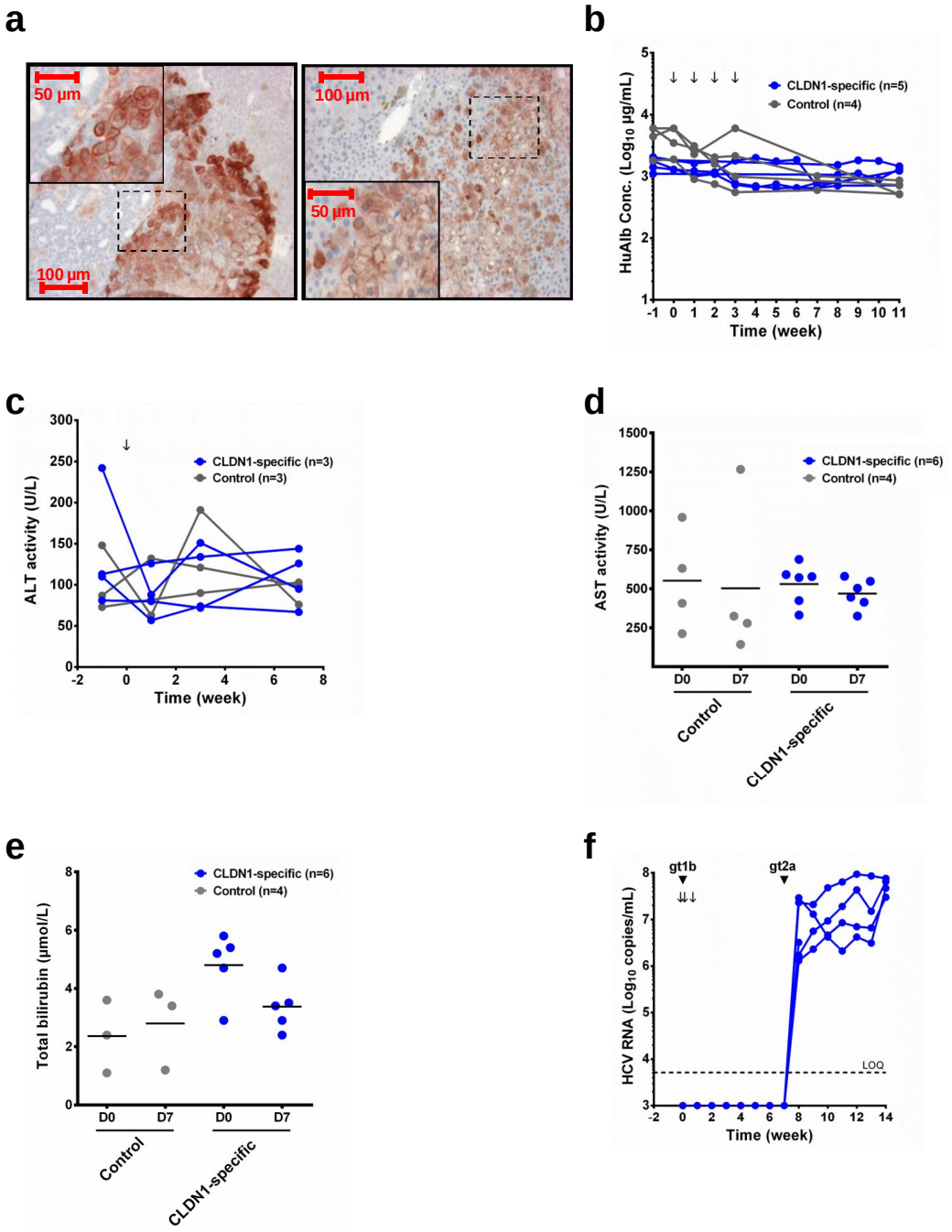

(**a**) Livers of chimeric mice from HCV-infected and control (left panel) or CLDN1-specific (right panel) mAb-treated mice were harvested, fixed in 4% formaldehyde and subjected to anti-human cytokeratin-18 (hCK18) immunostaining as described in Methods. Human hepatocytes were identified by anti-hCK18 immunostaining. Representative images for each group are shown (magnification 10x; inset 40x). (**b-e**) Human albumin (HuAlb) (**b**), ALT (**c**), AST (**d**) and total bilirubin (**e**) serum levels in CLDN1-specific (blue) or control (grey) mAb-treated mice. Each parameter remains stable following mAb injection ($p > 0.125$, Wilcoxon rank test). (**f**) Re-infection of protected mice. Animals treated with CLDN1-specific mAb and protected from HCV infection (genotype 1b) (see Fig. 2a) were re-inoculated with HCVcc Jc1 (genotype 2a). The rapid rise of viral load indicates that mAb-treated human hepatocytes are viable and fully permissive for HCV infection.

Supplementary Figure 7. Binding of CLDN1-specific mAb to primary mouse hepatocytes and mouse CLDN1.

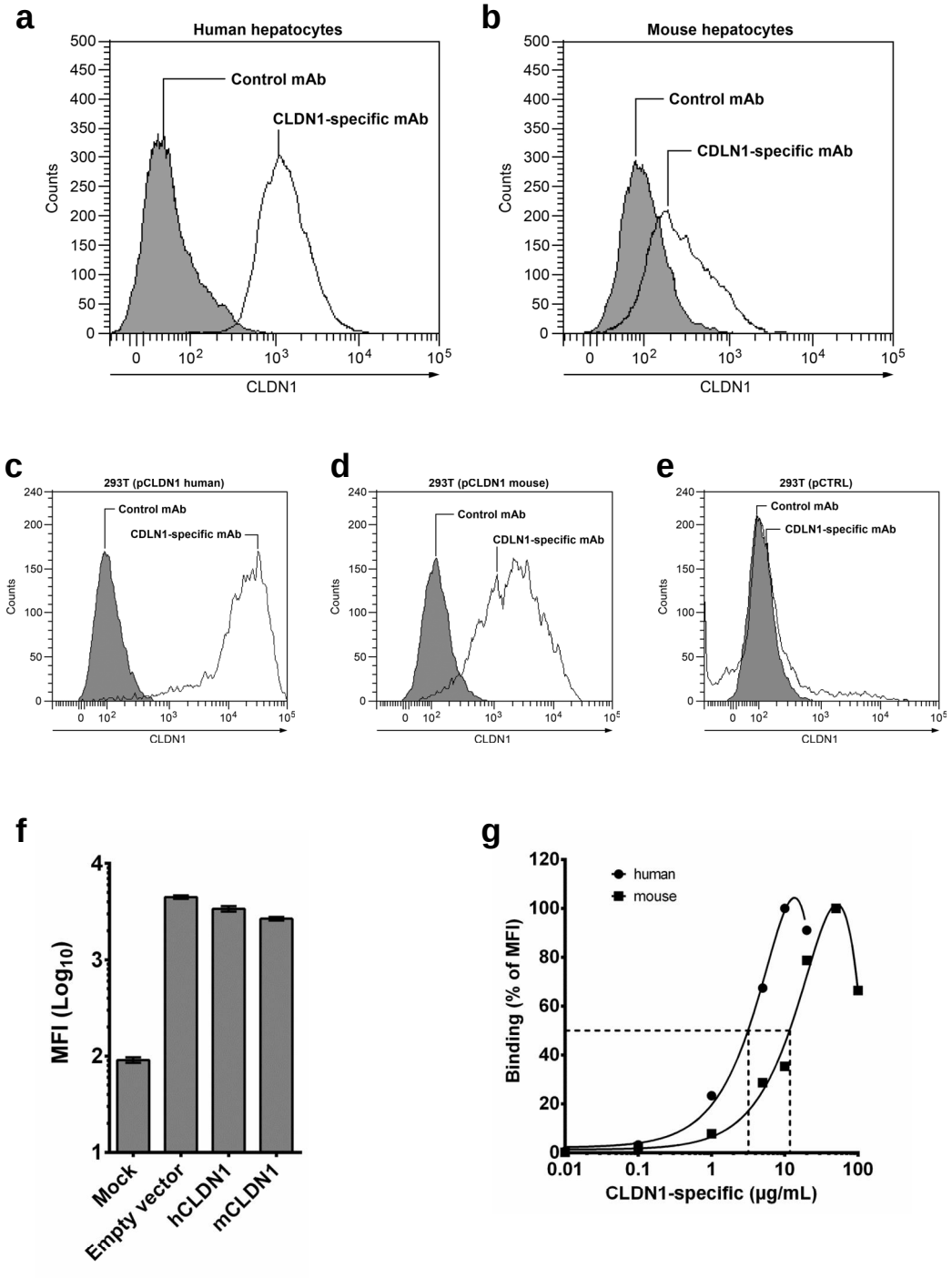

Primary (**a**) human or (**b**) mouse hepatocytes were incubated with 10 µg/mL of CLDN1-specific (black line) or control (grey) mAb. Binding was analyzed as described in Methods after incubation with PE-labeled anti-rat secondary antibody. (**c, d, e**) 293T-cells were transfected with plasmids encoding for (**c**) human or (**d**) mouse CLDN1 fused to cerulean fluorescent protein or (**e**) empty pTRIP-cerulean as described in Methods. Transfected cells were incubated with different amounts (0.01, 0.1, 1, 5, 10, 20, 50, 100 µg/mL) of CLDN1-specific or control mAb and the binding was revealed as in (**a**). The results are shown as histogram of cells incubated with 20

µg/mL of antibodies and gated in the cerulean positive cells. (**f**) Determination of transfection efficiency in 293T cells from (**c-e**) by quantification of the mean fluorescence intensity (MFI) of the cerulean tag. Results are expressed as means ± s.d (n=18) of one representative experiment out of 4 independent experiments. (**g**) Determination of the apparent Kd of CLDN1-specific mAb on human (black circles) and mouse (black squares) CLDN1 expressed in 293T cells (**c-e**). The PE median fluorescence intensity (MFI) was determined on the double cerulean-PE positive cells. The results are expressed as the % of MFI representing the specific binding of CLDN1-specific mAb and were used to determine the apparent Kd (dashed line). The results show one representative experiment out of 4 independent experiments.

Supplementary Figure 8. Biodistribution and absent adverse effects of CLDN1-specific mAb on intestine function.

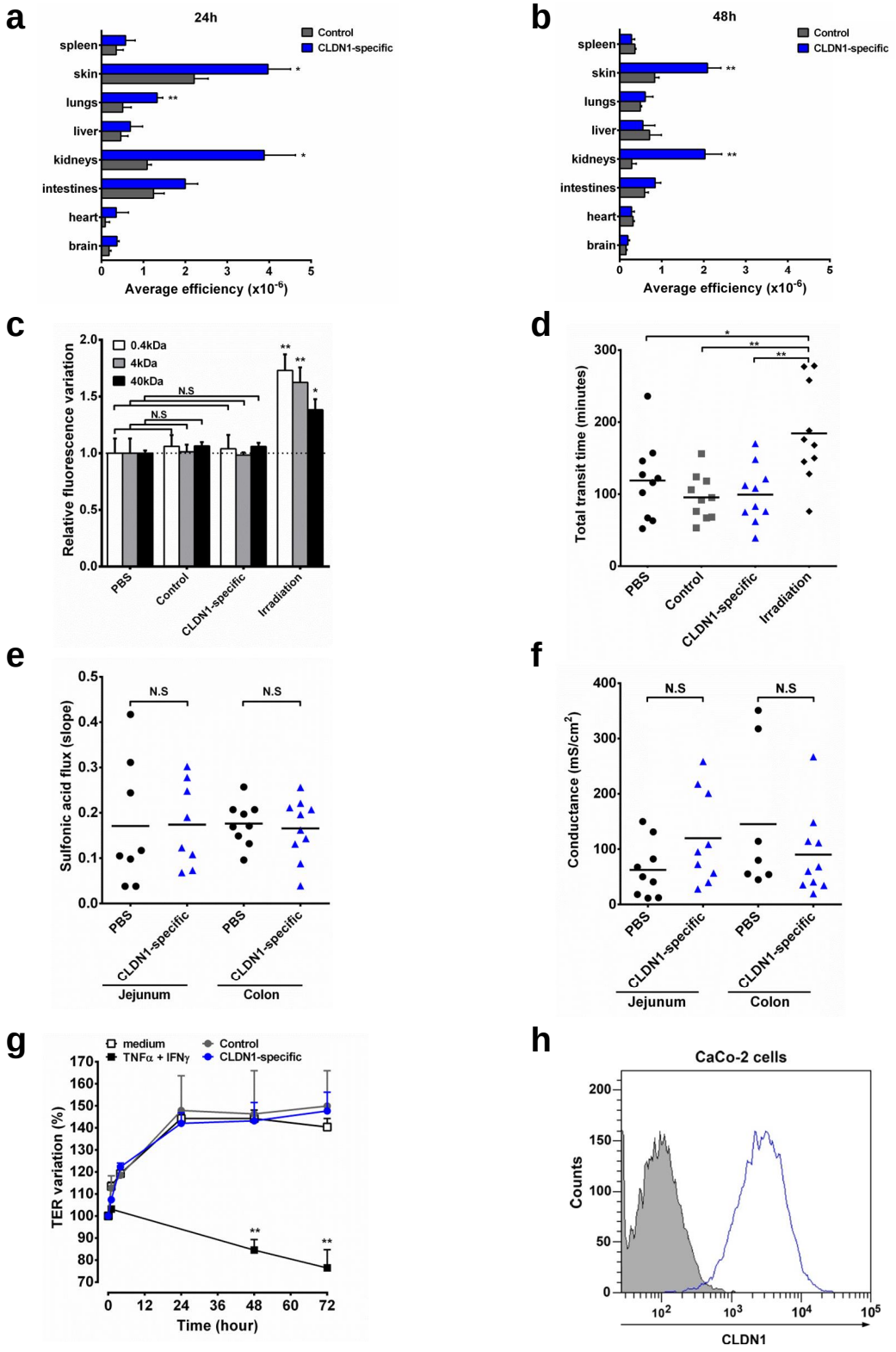

(**a, b**) *In vivo* biodistribution of the CLDN1-specific mAb in immunocompetent mice. Mice (n=6/group/time point) injected with 500 µg Alexa fluor 750-labeled control (grey bar) or CLDN1-specific (blue bar) mAb were sacrificed at 24 (**a**) and 48h (**b**). The

specific fluorescence was detected in each indicated organ using an IVIS Lumina 50 device with specific filter sets and expressed as average efficiency. The results show the mean ± s.e.m. from 6 mice. (**c**) CLDN1-specific mAb does not alter paracellular intestinal permeability in Balb/c mice *in vivo*. Intestinal permeability in mice (n=10 per group) was assessed 7 days after PBS, control or CLDN1-specific mAb injection (500 µg). Positive control mice received 15 Gy of X-ray 3 days prior to measurement. The paracellular intestinal permeability to 0.4 kDa fluorescein-sulfonic acid (white bars), 4 kDa FITC-Dextran (grey bars) and 40 kDa FITC-Dextran (black bars) were determined as described in Methods. Results are shown as fluorescence variation compared to the corresponding PBS group (mean of 10 mice ± s.e.m.). (**d**) Total intestinal transit time in Balb/c mice (n=10 per group). Mice were treated as in (**c**) with PBS (black circle), control (grey square) or CLDN1-specific (blue triangle) mAb. Seven days later mice were given carmine red by oral gavage (0.3 mg/g) and the total transit time was determined at the appearance of the first red fecal pellet. Positive control mice (black diamond) were treated as in (**c**). (**e, f**) Effect of CLDN1-specific mAb on *ex vivo* intestinal permeability (**e**) and conductance (**f**) in Balb/c mice. Mice (n=7-10 per group) were injected as in (**c, d**) and sacrificed 7 days later. Paracellular permeability to 0.4 kDa fluorescein-sulfonic acid (**e**) and conductance (**f**) of the jejunum and the colon of mice injected with PBS (black circle) or CLDN1-specific mAb (blue triangle) were determined in Ussingôs chambers as described in Methods. (**g**) *In vitro* trans-epithelial electrical resistance (TER). TER was determined at different time points on Caco-2 cells monolayers incubated without (medium, empty square) or with 100 µg/mL CLDN1-specific (blue circle) or control (grey circle) mAb, or a combination of 500 ng/mL of TNFα and IFNγ (black square). The results are shown as the TER variation in percentage of day 0 ± s.e.m from one representative experiment performed in triplicate. (**h**) CLDN1 expression on Caco-2 cells. Caco-2 cells were incubated with control (grey) or CLDN1-specific (blue line) mAb and analyzed by flow cytometry as described in Methods. (**d-f**) Results are shown as individual values for each mouse. The horizontal line indicates the mean. Arrows: antibody injection. N.S ï not significant, * $p < 0.05$, ** $p < 0.01$ (Mann-Whitney test (**a, b, e**), one-way ANOVA and Tukeyôs Post Hoc test (**d**), Kruskal-Wallis and Dunnôs Post Hoc test (**c, f**), Studentôs t-test (**g**)).

Supplementary Figure 9. Histopathology of organs in mice treated with CLDN1-specific mAb.

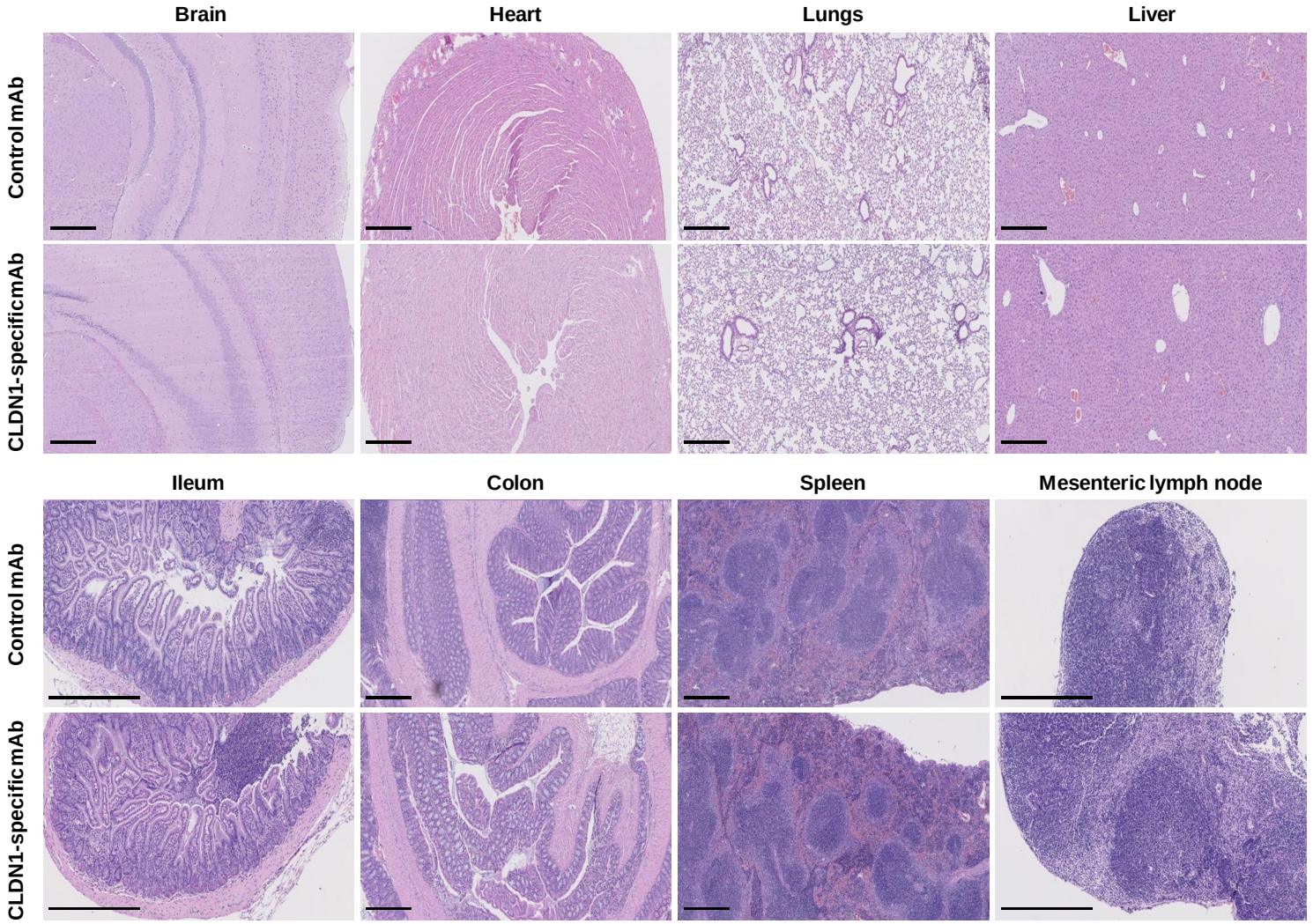

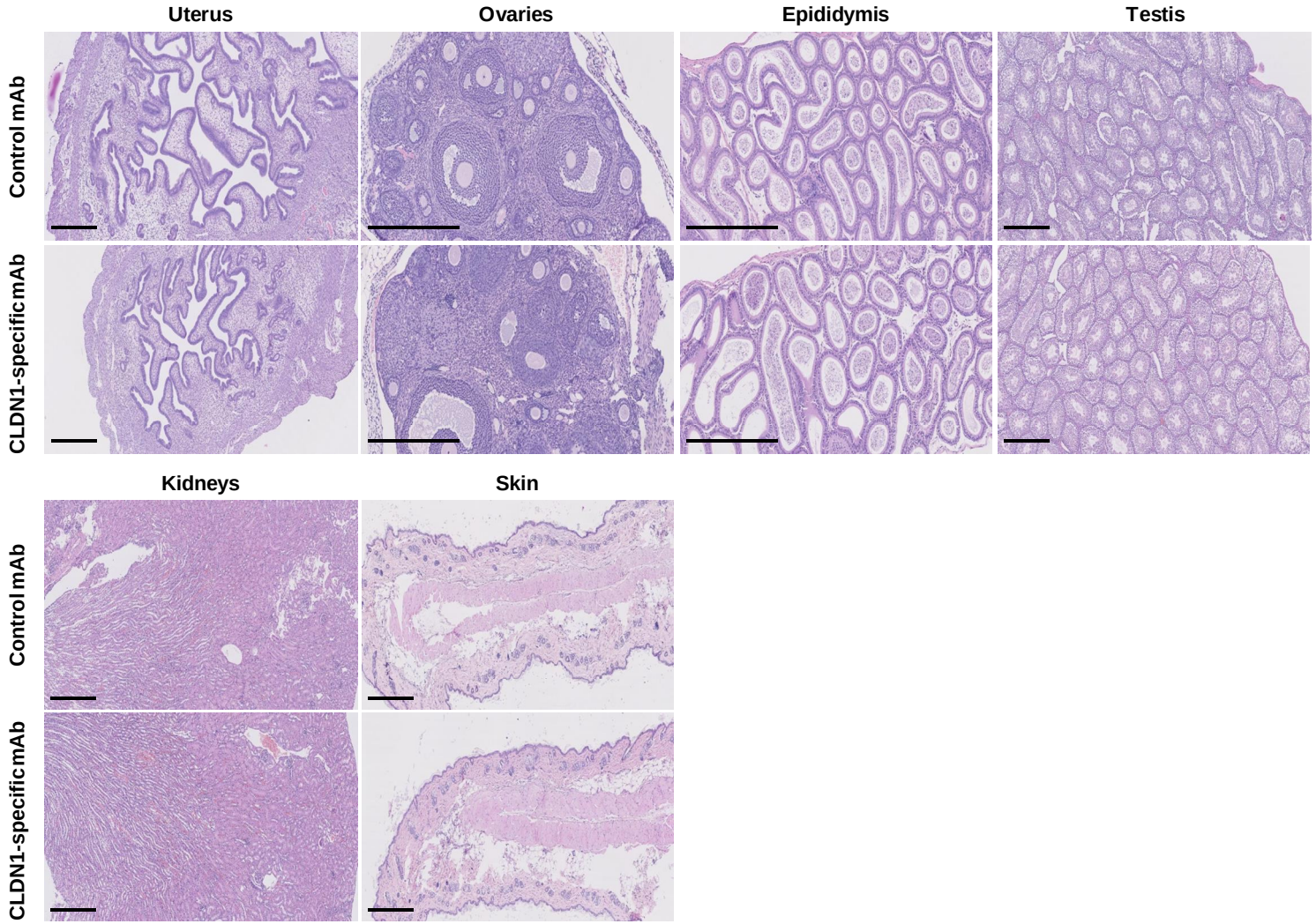

Balb/c mice received 500 µg of CLDN1-specific or control mAb. Seven days later, the organs were harvested, formalin-fixed, paraffin-embedded, cut and stained with hematoxylin-eosin. The samples were subjected to blinded histopathological analysis by a pathologist at the Institut Clinique de la Souris (ICS), Strasbourg. Scale bars ï 500 µm.

Supplementary Figure 10. Absent effect of CLDN1-specific mAb on tight junction integrity.

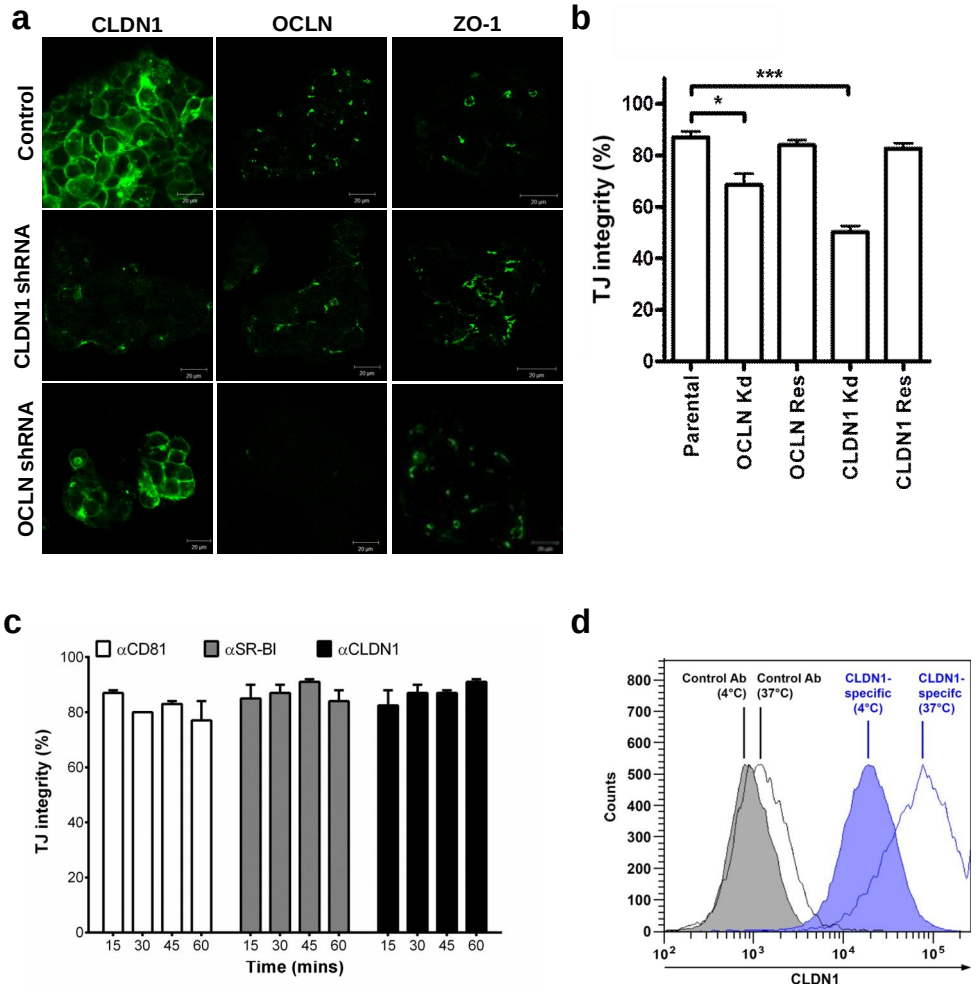

(**a**) CLDN1 silencing impairs TJ integrity. Parental HepG2 CD81, CLDN1 shRNA HepG2 CD81 and OCLN shRNA HepG2 CD81 cells were seeded on glass coverslips at $4x10^4$ cells/well and allowed to polarize for 5 days. Cells were stained with antibodies specific for CLDN1, OCLN or ZO-1 and visualized by confocal microscopy. Scale bar ï 20µm. (**b**) Rescue of CLDN1 silencing restore TJ integrity. Parental HepG2 CD81, CLDN1 shRNA HepG2 CD81 and OCLN shRNA HepG2 CD81 cells were grown for 5 days and TJ integrity was measured by incubating with CMFDA, which measures barrier function. TJ integrity was determined by quantifying the number BC which retained CMFDA in 10 fields of view on 3 replicate coverslips. Restriction of CMFDA to the BC indicate that polarized HepG2 cells have functional TJs ± s.d. (**c**). CLDN1-specific mAb does not impact TJ functionality. Polarized HepG2 CD81 cells (5 day culture) were treated with 10 µg/mL anti-CD81 (2s131), anti-SR-BI (P72) or CLDN1-specific mAb for 1h. During the hour incubation, TJ integrity was determined by quantifying the number BC which retained CMFDA in 10 fields of view on 3 replicate coverslips at 15 min intervals. Restriction of CMFDA to the BC indicate that polarized HepG2 cells have functional TJs ± s.d. (d) CLDN1-specific mAb does not induce CLDN1 internalization. Huh7.5.1 cells were incubated with control (grey) or CLDN1-specific (blue) mAb for 1h at 4 (solid body) or 37°C (empty body). CLDN1-specific mAb binding was analyzed by flow cytometry as described in Methods. * p <0.01, ** p <0.001, *** p <0.0001 (Studentôs t-test).

Supplementary Figure 11. Antiviral mechanism of action mediated by the CLDN1-specific mAb.

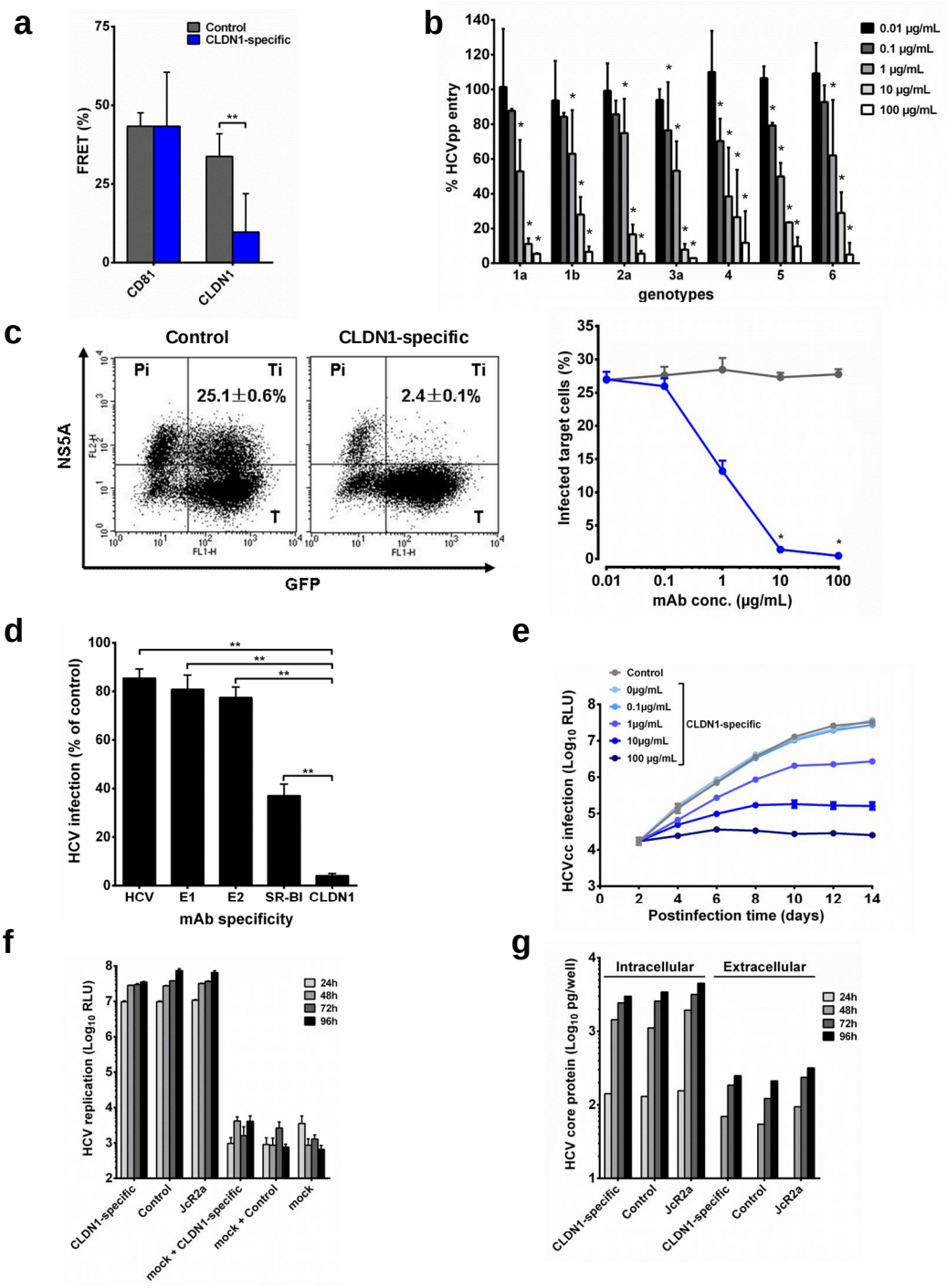

(**a**) CLDN1-specific mAb specifically inhibits CD81-CLDN1 co-receptor interactions. FRET analysis of CD81-CD81 (left) and CD81-CLDN1 (right) co-receptor interactions in 293T cells expressing tagged entry factors incubated with control (grey bars) or CLDN1-specific (blue bars) mAb (10 µg/mL). Results are indicated as the means ± s.d. of 10 independent experiments. (**b**) Pan-genotypic antiviral activity of CLDN1-specific mAb in HCVpp infected primary human hepatocytes. Primary human hepatocytes were pre-incubated with increasing concentrations of CLDN1-specific mAb for 1h at 37°C before infection with HCVpp bearing the E1E2 glycoproteins from

genotypes 1-6. Lentivirus-based HCVpp bearing envelope glycoproteins of strains H77 (genotype 1a), HCV-J (1b), JFH1 (2a), UKN3A1.28 (3a), UKN4.21.16 (4), UKN5.14.4 (5) and UKN6.5.340 (6) were produced as described[4]. The results are expressed as the percentage of HCVpp entry in the presence of CLDN1-specific mAb compared to HCVpp entry in the presence of the control mAb (=100%). Means ± s.d. from three independent experiments in duplicate using hepatocytes from three different donors are shown. (**c**) Inhibition of cell-cell transmission by CLDN1-specific mAb. NS5A+ HCV producer cells (Pi) and target GFP-expressing cells (T) were co-cultivated with an anti-E2 mAb (AP33, 25 µg/mL) to block cell-free transmission. Cell-cell transmission was determined by quantification of GFP+ NS5A+ target cells (Ti) in presence of CLDN1-specific or control mAb by flow cytometry (left panel) as described[5]. Cell-cell transmission (Ti), not affected by control mAb (grey circles, right panel), is dose dependently inhibited by CLDN1-specific mAb (blue circles, right panel). Means ± s.d. of three independent experiments performed in duplicate are shown. (**d**) Quantification of infected Ti cells during treatment with HCV- or entry factor-specific antibodies by flow cytometry. The results show the percentage of HCV infection compared to control mAb (means ± s.d. from three independent experiments in triplicate). (**e**) Effect of CLDN1-specific mAb on viral spread. HCVcc infection of Huh7.5.1 cells incubated with CLDN1-specific or isotype control mAb 48h after infection at the indicated concentrations. Medium with mAbs was replenished every 3-4 days. Means ± s.d. from one representative experiment performed in triplicate is shown. (**f**, **g**) CLDN1-specific mAb does not impair HCV replication and assembly/release. (**f**) HCV replication. Huh7.5 cells with a stable knock-down of CD81 (Huh7.5 shCD81.1) were transfected with *in vitro* transcripts of JcR2a. Eight hours later, CLDN1-specific or control mAb (100 µg/mL) was added. Cells were lysed 24, 48, 72 and 96h later to quantify Renilla luciferase expression, a marker for HCV RNA replication. Non-transfected cells with or without antibody and transfected cells without antibody served as negative and positive controls, respectively. (**g**) HCV assembly/release. Cell lysates (intracellular) and supernatants (extracellular) from (**f**) were used to measure HCV core protein amounts as described in Methods. RLU: relative light units. Cell viability was determined by using MTT (3-(4,5-dimethylthiazol-2-yl)-2,5-diphenyltetrazolium bromide) assay and did not differ between CLDN1-specific and control mAb-treated cells (data not shown). *$p < 0.01$, **$p < 0.0001$ (Student's t-test).

Supplementary Figure 12. miRNA profiling in mock and HCV-infected Huh7.5.1 cells treated with CLDN1-specific or control antibody.

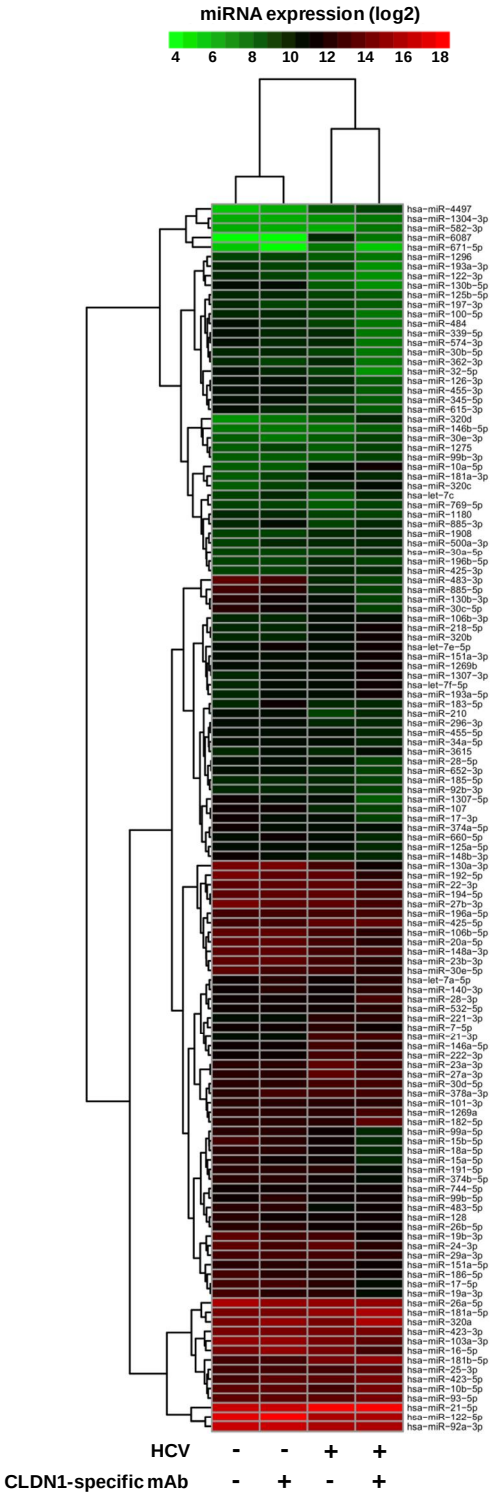

Ten days following initiation of infection, mock or HCV Jc1-infected Huh7.5.1 cells were treated for 24h with 100 µg/mL CLDN1-specific or control mAb. Cells were harvested and subjected to miRNA profiling. The heatmap shows hierarchical clustering of the different samples and of the 100 most abundant miRNAs in each sample on the basis of their expression. High relative miRNA expression (Log_2-transformed) is indicated by red shades, low expression by green shades.

Supplementary Figure 13. Full length immunoblots from Figure 3.

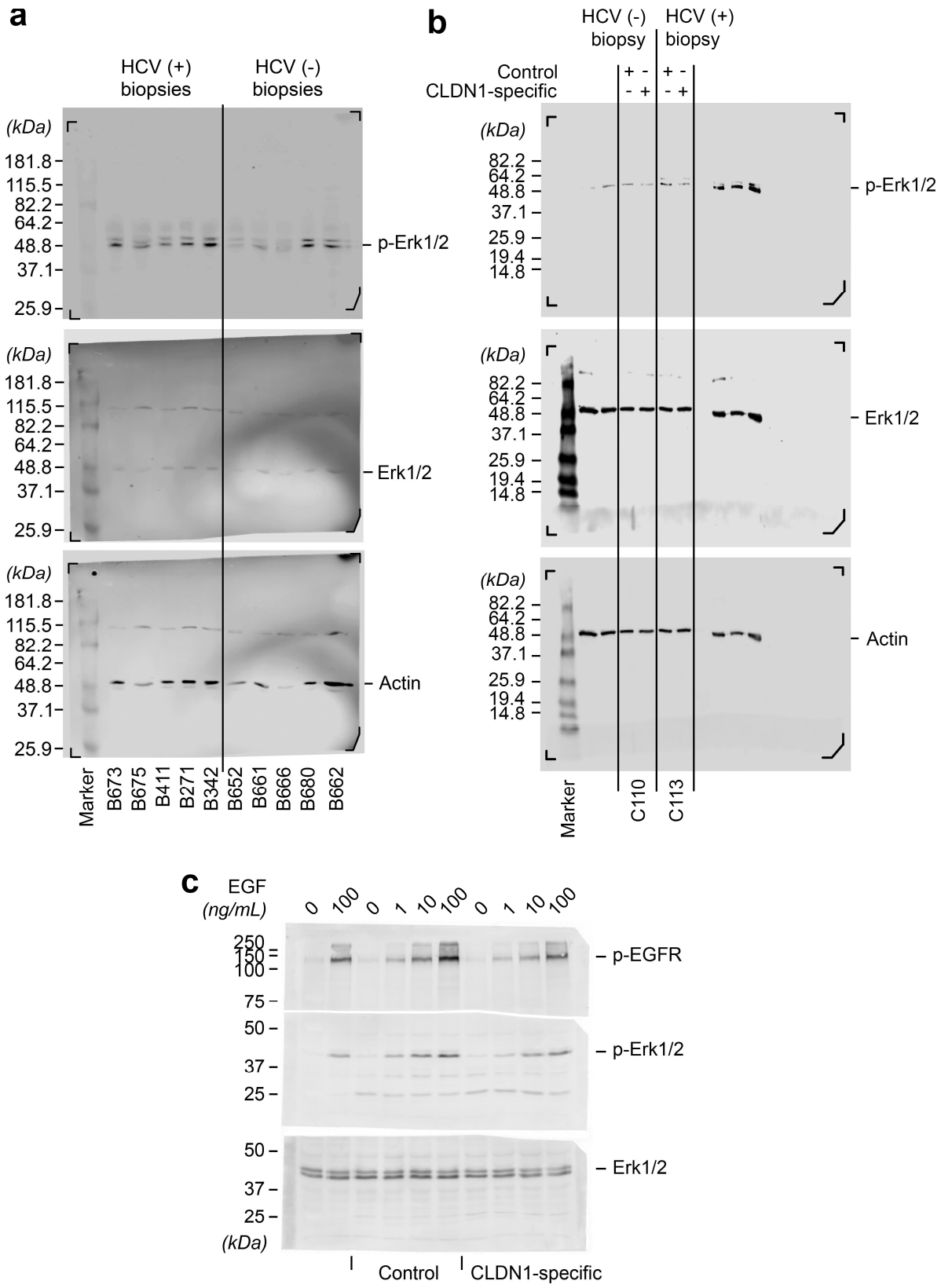

To demonstrate the specificity of the ERK1/2, p-ERK1/2, and p-EGFR-specific antibodies for analyses of liver biopsies and liver cell lysates representative full length gels are shown for (**a**) figure 3c, (**b**) figure 3f, (**c**) figure 3g. (**a, b**) Reducing 10%

SDS-PAGE gel electrophoresis of liver biopsy lysates. Blotting membranes were first probed for p-ERK1/2 (upper blot; Phospho-p44/42 MAPK (ERK1/2) (Thr202/Tyr204) (E10) mouse mAb, Cell Signaling) and then re-probed for total ERK1/2 (middle blot; p44/42 MAPK (ERK1/2) rabbit pAb, Cell Signaling) and actin (lower blot; beta-actin (AC-15) mouse mAb, Sigma). Secondary antibodies were IRDye 800CW-conjugated goat anti-rabbit (for p-ERK1/2) and IRDye 680-conjugated goat anti-mouse IgG (for actin and ERK1/2). Fluorescence intensities were measured and processed to black/white images using the Odyssey Infrared Imaging System (LI-COR). Identified proteins are indicated on the right. The MW (kDa) of protein markers (BenchMark Prestained protein ladder, Invitrogen) is indicated on the left. (**c**) Reducing 10% SDS-PAGE gel electrophoresis of Huh7.5.1 cell lysates. For protein detection the blotting membrane was cut between the 50 and 75 kDa protein marker and probed for p-EGFR (>75 kDa membrane; upper blot) (Anti-p-EGFR (pTyr1086), rabbit pAb, Sigma) and p-ERK1/2 (<50 kDa membrane; middle blot) (Phospho-p44/42 MAPK (ERK1/2) (Thr202/Tyr204) (E10) mouse mAb, Cell Signaling). The <50 kDa membrane (lower blot) was then re-probed for total ERK1/2 (p44/42 MAPK (ERK1/2) rabbit pAb, Cell Signaling). Secondary antibodies were goat anti-mouse-AP (for p-ERK1/2 and actin) and goat anti-rabbit-AP (for p-EGFR). Fluorescence intensities were measured and processed to black/white images using the Typhoon Trio high performance fluorescence scanner (GE Healthcare). The MW (kDa) of protein markers (Precision Plus Protein Standards All Blue, BioRad) are indicated. Identified proteins are indicated on the right. Contrasts of images shown in figure 3 were equally adjusted for entire membranes before cropping using the Adobe Photoshop software.

Supplementary Figure 14. Mathematical model of CLDN1-specific mAb treatment and viral load decline.

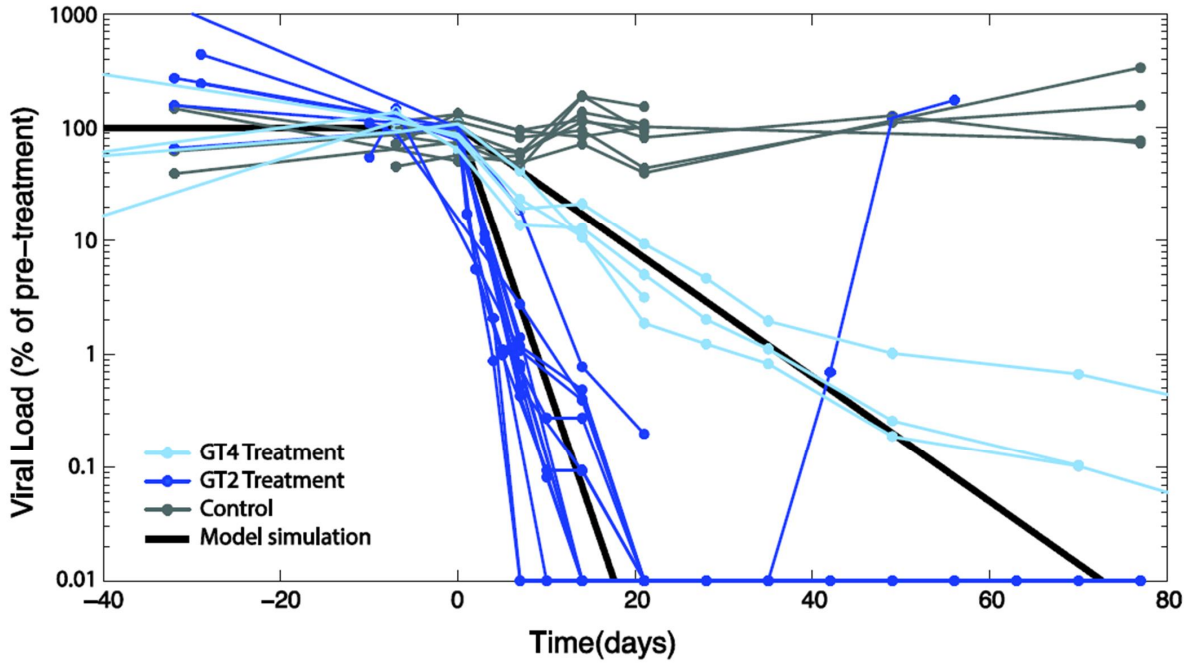

Experimental measurements of viral load over time in control (grey) and CLDN-1-specific mAb-treated mice (blue). Time courses were normalized to the pre-treatment viral load and are shown as % of pre-treatment levels on a logarithmic scale; measurements taken in the same mice are connected by lines. The mathematical model by Neumann *et al.*[6] was used to simulate decline of viral load. Model simulation results are shown as a solid black line in the plot. The key parameter determining the slope of the decline is the infected cell death rate, here estimated to yield an infected cell half-life of around 1.3 days for genotype 2a (dark blue) and 5.4 days for genotype 4 (light blue). The virion clearance rate used in the simulation is c=6.3, infection inhibitor efficacy **ɖ**=99%. Other model parameters (s, d, **ɓ**, **ɟ**) are determined by the pre-treatment steady state levels and do not need to be estimated explicitly.

Supplementary Figure 15. Apoptosis in HCV-infected Huh7.5.1 cells and kinetics of persistently infected Huh7.5.1 cells.

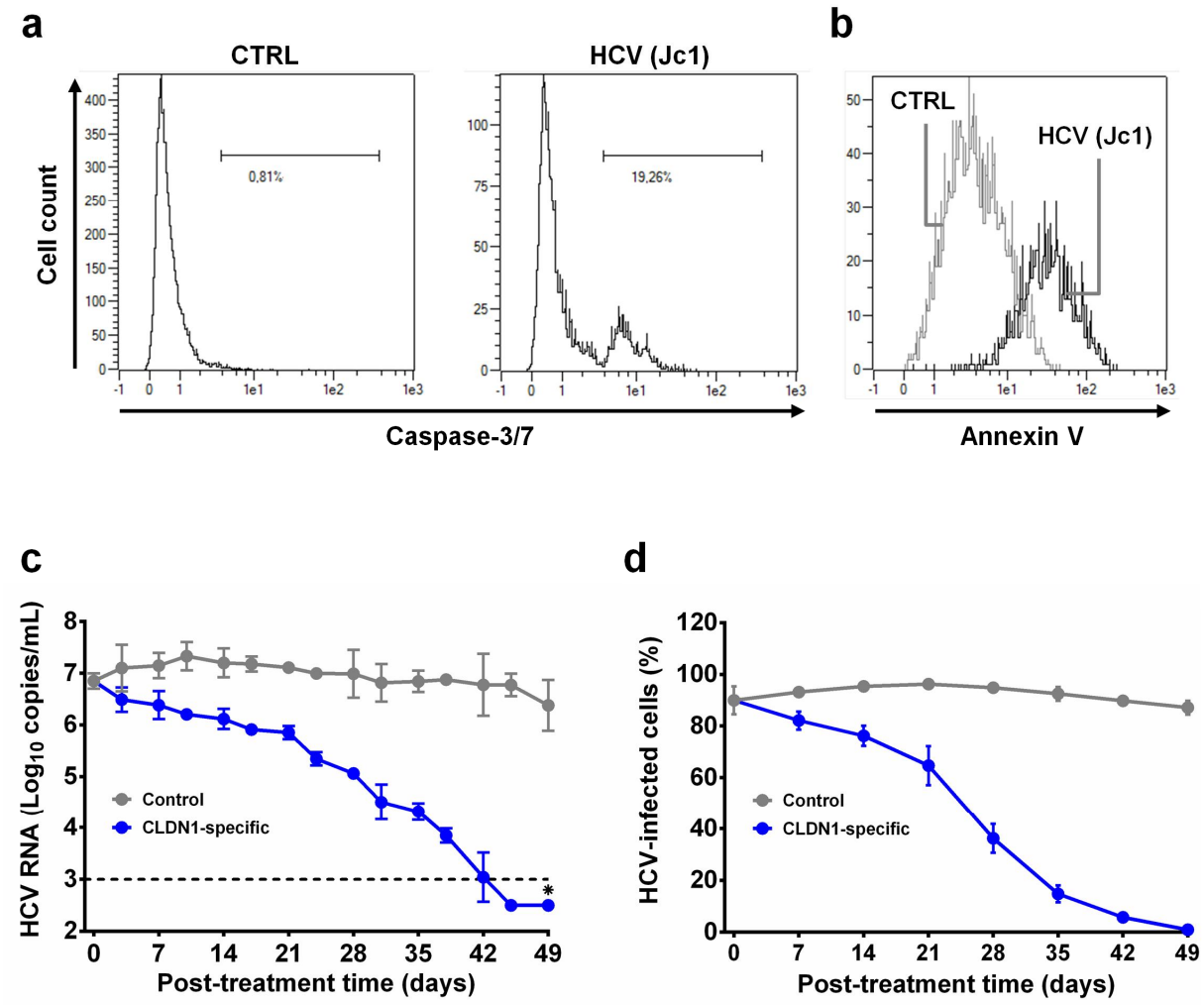

(**a, b**) Analysis of apoptosis in persistently HCV infected cells. Persistent HCV infection was established by transfection of HCV RNA (Jc1) into Huh7.5.1 cells. One week after electroporation of HCV RNA, cells were stained for activated caspase-3/7 (**a**) or incubated with labeled annexin V (**b**) as described in Methods. Mock-transfected cells were analyzed in parallel and served as a negative control (CTRL). (**c, d**) CLDN1-specific mAb (100 µg/mL) leads to eradication of HCV-infected cells in a time-dependent manner. Huh7.5.1 cells were electroporated with HCV RNA (Jc1) to establish persistent infection. One week later, cells were continuously incubated with 100 µg/mL control or CLDN1-specific mAb as described in Methods. HCV RNA (**c**) was quantified by RT-PCR (dashed line - limit of detection 10^3 copies/mL)[7]. The percentage of HCV-infected cells (**d**) was determined by flow cytometry of permeabilized cells harvested at different time points and stained with an HCV E2-specific mAb (AP33) followed by a PE-conjugated anti-mouse IgG (BD Bioscience) as described[8]. *Eradication of HCV RNA was confirmed using the clinically licensed Abbott Real Time HCV assay (sensitivity 120 IU HCV RNA/sample).

SUPPLEMENTARY TABLES

Supplementary Table 1: Protocol, genotype of inoculum, injected antibody and viral load pre- and post antibody administration of individual chimeric mice.

Protocol	Genotype	mAb	Mouse ID	VL begining of treatment (x 10^6 copies/mL)	VL end of treatment (x 10^6 copies/mL)
Prevention	1b	Control	101	Negative	**4.4**
			102	Negative	**10**
			103*	Negative	**2.1**
			104	Negative	**8.2**
		CLDN1-specific	201	Negative	Negative
			202	Negative	Negative
			203	Negative	Negative
			204	Negative	Negative
			205	Negative	Negative
	4	Control	3484	Negative	**56.1**
			3487	Negative	**11**
			3520	Negative	**4.01**
			3525	Negative	**72.7**
		CLDN1-specific	3485	Negative	Negative
			3489	Negative	Negative
			3490	Negative	Negative
			3493	Negative	Negative
			3496	Negative	Negative
Treatment	2a/2a	Control	1491	**2.39**	**14**
			1492	**0.97**	**1.33**
			1493	**4.71**	**2.76**
			1494	**3.89**	**2.14**
		CLDN1-specific	1406	**0.89**	**1.84**
			1451	**1.61**	Negative
			1452	**1.90**	Negative
			1994	**0.86**	Negative
			1996	**0.28**	Negative
	1b/2a	Control	4718	**1.14**	**2.33**
			6464	**1.76**	**2.11**
			6470	**5.1**	**2.01**
		CLDN1-specific	3125	**1.58**	Negative
			3256	**2.06**	Negative
			3345	**3.51**	**18**
			3377	**1.73**	Negative
			3524	**0.46**	Negative
	2a	Control	6403	**2.17**	**1.12**
			6404	**1.85**	**3.43**
			6405	**3.88**	**7.43**
			6415	**4.55**	**2.38**
		CLDN1-specific	6776	**1.86**	Negative
			6777	**1.88**	Negative
			6778	**6.59**	Negative
			6779	**0.25**	Negative
			6782	**5.49**	Negative
			6783	**6.32**	Negative
	4	CLDN1-specific	3484	**56.1**	**0.19**
			3487*	**11**	**0.18**
			3520	**4.01**	Negative
			3525*	**72.7**	**21.2**

*VL: Viral load; *mouse died before end of treatment protocol. A negative value indicates a viral load below the limit of quantitation or absence of serum HCV RNA.*

Supplementary Table 2: Biochemical parameters analyzed in serum of Balb/c mice treated with control or CLDN1-specific mAbs.

	Sex	ALT (48h) U/L	Urea mM	Total proteins g/L	Albumin g/L	Total bilirubin µM	LDH U/L	AST U/L	ALT U/L	ALP U/L	Creatinin µM
Control	M	36	12.1	45	24	1.5	440	58	39	125	10.8
		40	8.3	45	25	1.5	505	80	38	122	11.6
		37	8.3	45	25	1.7	341	55	37	134	12.9
		41	7.9	48	26	1.9	546	65	35	128	11.3
		77	10.9	44	24	1.4	456	88	39	128	13.0
	F	44	8.5	48	28	2.1	447	73	39	147	12.9
		39	7.5	45	26	1.1	527	80	38	128	12.6
		29	8.3	47	27	1.5	494	61	33	141	16.6
		42	7.8	48	29	2.1	352	69	43	145	15.9
		37	8.6	46	27	1.9	380	94	46	170	17.3
	Mean	**42.20**	**8.82**	**46.10**	**26.10**	**1.67**	**448.80**	**72.30**	**38.70**	**136.80**	**13.48**
	s.e.m	4.08	0.47	0.48	0.53	0.10	22.76	4.13	1.16	4.58	0.72
CLDN1-specific	M	37	8.9	46	26	1.9	462	60	43	129	11.0
		40	8.7	46	25	1.9	495	46	28	117	12.9
		61	7.0	45	23	1.2	780	121	32	96	10.1
		38	11.0	45	24	0.6	692	83	39	127	16.7
		44	10.2	43	22	1.2	457	43	33	74	16.7
	F	31	9.2	49	28	2.2	296	55	31	142	14.0
		28	8.4	46	27	1.8	310	69	28	144	14.6
		62	13.8	45	26	1.8	401	163	54	152	22.1
		33	9.4	44	26	1.4	845	120	72	140	15.7
		29	7.5	45	27	1.7	302	56	27	135	13.5
	Mean	**40.30**	**9.41**	**45.40**	**25.40**	**1.57**	**504.00**	**81.60**	**38.70**	**125.60**	**14.73**
	s.e.m	3.87	0.61	0.50	0.60	0.15	63.61	12.65	4.55	7.62	1.07
	***p*-value**	***0.54***	***0.26***	***0.41***	***0.54***	***0.73***	***0.91***	***0.79***	***0.29***	***0.57***	***0.38***

ALT, alanine transaminase; LDH, lactate dehydrogenase; AST, aspartate transaminase; ALP, alkaline phosphatase. p-value (control versus CLDN1-specific mAb treated group) determined by Student's t-test.

Supplementary Table 3: Hematological parameters analyzed in serum of Balb/c mice treated with control or CLDN1-specific mAbs.

	Sex	WBC x10^3 cells/µL	RBC x10^6 cells/µL	HGB g/dL	HCT %	MCV fL	MCH pg	MCHC g/dL	Neutro %	Lympho %	Mono %	Eosino %	LUC %	Baso %	PLT x10^3 cells/µL	MPV fL
Control																
	M	6.78	9.74	14.2	49.0	50.3	14.7	29.2	18.7	70.9	2.5	6.9	0.9	0.1	1062	4.0
		9.08	9.86	14.6	50.4	51.2	14.8	29.0	18.0	76.8	2.2	2.3	0.6	0.1	1216	3.9
		9.42	10.02	14.8	51.4	51.2	14.8	28.8	13.6	81.5	2.3	1.9	0.6	0.0	1158	3.8
		7.60	8.32	11.0	43.0	51.5	13.2	25.7	16.9	77.2	1.0	3.7	1.0	0.2	1030	4.0
	F	7.22	9.50	14.6	48.2	50.7	15.4	30.4	15.2	74.6	1.6	7.7	0.8	0.1	946	3.9
		6.28	8.48	12.8	43.2	51.1	15.0	29.4	23.4	65.5	1.7	9.0	0.4	0.0	648	4.2
		5.44	9.22	13.4	47.4	51.3	14.5	28.3	16.6	80.1	1.1	1.9	0.3	0.0	1136	3.8
		7.34	9.40	14.0	49.2	52.2	14.9	28.5	15.4	80.2	1.3	2.4	0.7	0.1	1058	3.9
		8.50	9.26	14.2	49.6	53.5	15.4	28.8	12.8	82.7	0.8	3.1	0.6	0.0	1150	3.9
	Mean	**7.52**	**9.31**	**13.73**	**47.93**	**51.44**	**14.74**	**28.68**	**16.73**	**76.61**	**1.61**	**4.32**	**0.66**	**0.07**	**1044.89**	**3.93**
	s.e.m	0.43	0.19	0.40	0.99	0.31	0.22	0.42	1.05	1.85	0.20	0.92	0.07	0.02	56.45	0.04
CLDN1-specific																
	M	6.28	9.08	12.8	46.6	51.2	14.0	27.4	21.2	74.3	1.3	2.7	0.4	0.1	1394	3.9
		10.88	9.38	13.2	48.4	51.7	14.2	27.4	33.6	60.9	2.3	1.6	1.7	0.0	1454	4.2
		8.16	8.46	12.8	43.8	51.7	15.0	29.0	20.7	66.0	3.0	8.7	1.4	0.1	602	4.2
		12.76	9.36	13.6	48.4	51.7	14.6	28.3	45.2	45.3	3.1	2.9	3.4	0.0	1302	3.9
	F	6.72	9.84	14.8	49.0	49.8	14.9	30.0	16.9	75.2	1.9	5.3	0.6	0.0	970	3.8
		6.90	9.40	14.2	48.8	51.8	15.1	29.1	15.2	81.5	1.6	1.3	0.3	0.1	1078	3.8
		8.56	9.02	13.6	47.2	52.3	15.1	28.8	15.3	81.4	1.0	1.7	0.6	0.1	1010	3.9
		7.02	9.00	14.2	47.4	52.6	15.8	30.0	21.7	70.5	1.0	6.3	0.5	0.0	882	4.1
		7.10	9.50	14.2	48.2	50.8	14.9	29.3	16.2	80.8	1.2	1.4	0.3	0.1	868	3.8
	Mean	**8.26**	**9.23**	**13.71**	**47.53**	**51.51**	**14.84**	**28.81**	**22.89**	**70.66**	**1.82**	**3.54**	**1.02**	**0.06**	**1062.22**	**3.96**
	s.e.m	0.73	0.13	0.23	0.54	0.28	0.18	0.32	3.37	3.96	0.27	0.88	0.34	0.02	92.39	0.06
	***p*-value**	***0.83***	***0.48***	***0.62***	***0.31***	***0.42***	***0.76***	***0.93***	***0.16***	***0.31***	***0.69***	***0.29***	***0.89***	***0.84***	***0.86***	***1.00***

WBC, white blood cells; RBC, red blood cells; HGB, hemoglobin; HCT, hematocrit; MCV, mean corpuscular volume; MCH, mean corpuscular hemoglobin; MCHC, mean corpuscular hemoglobin concentration; LUC, large unstained cells; PLT, platelets; MPV, mean platelet volume. Grey lines indicate mice not tested because of blood coagulation. p-value (control versus CLDN1-specific mAb treated group) determined by Student's t-test.

Supplementary Table 4: Characteristics of the patients and patient-derived biopsies studied in Fig. 3.

Biopsy ID	HCV genotype	Viral load (IU/mL)	Diagnosis	Metavir	Age (Years)	Gender
B673	4	439,039	Chronic HCV infection	A1/F1	49	M
B675	3a	672,811	Chronic HCV infection	A2/F2	49	M
B411	2	7,079,458	Chronic HCV infection	A2/F2	53	F
B271	1a	5,800,000	Chronic HCV infection	A3/F1	52	F
B342	3a	1,757,349	Chronic HCV infection	A3/F2-3	50	F
B652	N/A	N/A	Normal liver	N/A	39	F
B661	N/A	N/A	NAFLD	N/A	59	M
B666	N/A	N/A	NAFLD	N/A	27	M
B680	N/A	N/A	Steatosis	N/A	44	M
B662	N/A	N/A	Drug-induced liver injury	N/A	62	F
C142	1a	10,700,500	Chronic HCV infection	A2/F4	57	F
C140	1a	4,237,018	HCV and HIV co-infection	A1/F1	41	F
C114	1a	1,174,898	Chronic HCV infection	A1/F1	44	M
C94	1b	564,659	Chronic HCV infection	A2/F4	51	M
C80	1b	2,750,801	Chronic HCV infection	A2/F3	41	F
C29	N/A	N/A	Normal liver	N/A	61	M
C28	N/A	N/A	Normal liver	N/A	50	F
C19	N/A	N/A	Primary biliary fibrosis	N/A	62	F
C98	1a	6,000,000	HCV + HIV	A1/F2	33	M
C106	4a/c/d	941,734	HCV	A1/F2	51	M
C113	1b	17,875	HCV	A2/F4	62	F
C95	N/A	N/A	Granulomatosous hepatitis (sarkoidosis), resoluted HCV	N/A	35	M
C110	N/A	N/A	NASH/ASH	N/A	55	M
C115	N/A	N/A	NASH/ASH	N/A	57	M

NASH, nonalcoholic steatohepatitis; ASH, alcoholic steatohepatitis; NAFLD, nonalcoholic fatty liver disease; N/A, not applicable.

Supplementary Table 5: Half maximal inhibitors concentrations (IC_{50}) on HCVcc Luc-Jc1 infection and half maximal cytotoxic concentrations (CC_{50}) of protein kinase inhibitors (PKIs) in Huh7.5.1 cells.

Compound	IC_{50} (µM)	CC_{50} (µM)
Erlotinib	5 ± 0.9	>100
UO126	12.5 ± 3.2	>100

Dose-dependent infection was measured using luciferase reporter gene assay and toxicity of PKIs was measured using Prestoblue assay as described in Methods. IC_{50} and CC_{50} derived by extrapolation from three independent experiments performed in triplicates are represented as median (± standard error of median).

SUPPLEMENTARY METHODS

Transmission electron microscopy (TEM) analyses of tight junctions. For TEM analyses, mouse livers were fixed in 2.5% glutaraldehyde and 2.5% formaldehyde in cacodylate buffer (0.1 M, pH 7.4). The samples were post fixed in 1% osmium tetroxide in 0.1 M cacodylate buffer for 1h at 4°C and dehydrated through graded alcohol (50, 70, 90, 100%) and propylene oxide for 30 min each. As a positive control, healthy human liver tissue was processed using the same protocol. Human liver tissue was obtained after informed consent from patient undergoing liver resection for metastasis of breast cancer without clinical evidence for liver disease and absent HCV, HBV or HIV infection. Use of human liver tissue for research purposes had been approved by the local ethics committee. Fixed mouse or human liver samples were embedded in Epon 812. Ultrathin sections were cut at 70 nm, contrasted with uranyl acetate and lead citrate, and examined at 70 kV with a Morgagni 268D electron microscope. Images were captured digitally by Mega View III camera (Soft Imaging System). Lipofuscin, a typical hallmark frequently present in human hepatocytes and not easily detectable in mouse hepatocytes[1,2], was used to localize human hepatocytes. A large series of TEM images was analyzed by blind analysis.

Amplification and cloning of HCV E1E2 derived from isolated serum HCV RNA from infected mice. Total RNA was purified from mouse serum and cDNA was synthesized as described[4,9]. The cDNA was used as the template for PCR amplification as described[9,10]. Full-length E1E2 PCR products were cloned into PCR 2.0-TOPO (Invitrogen). Following sequencing (GATC Biotech), cDNA containing the full-length E1E2 coding sequence was digested by *Eco*RV and subcloned into expression vector pCMV-IRES for production of HCVpp[9,10]. For HCVcc, the E1E2 sequences were transferred into JCR2a[11] in a 4-fold-ligation using the restriction enzymes *Nsi*I, *Sal*I, *Not*I and *Afe*I. The correctness of the inserts was confirmed by sequencing.

HCVcc production and infection. Huh7.5 cells were electroporated with 10 µg RNA of each HCV variant encoding for envelopes isolated from mouse serum. After 48, 72 and 96h supernatants were collected, 0.45 µM filtered and stored at +4°C. Cell culture supernatants were concentrated with Centricon Plus-70 columns (Millipore, #UFC710008). For determination of viral titers, $TCID_{50}$ were determined after cell staining by immunohistochemistry as described[12]. For inhibition studies, HCVcc containing mouse serum-derived envelopes were mixed with CLDN1-specific or control antibodies for 30 min at different concentrations and added to Huh7.5 cells (MOI 1) cultured in 96-well-plates. Incubation of Huh7.5 cells with viruses and antibodies was stopped 6h later by replacing the virus with fresh medium. 72h later, HCV infection was determined by luciferase reporter activity.

Pseudoparticle production and infection. VSV, HCV and non-enveloped pseudoparticles (pp) were produced as described[4,9]. HCVpp were added to Huh7.5.1[13], 293T[9] or 293T stably expressing CLDN1[14] cells or human hepatocytes[5]. HCVpp entry was determined by analysis of luciferase reporter gene expression as described[9]. To study antibody-mediated inhibition of HCV infection, Huh7.5.1 cells or primary human hepatocytes were preincubated with antibodies and infected as described[4].

Analysis of claudin-1, 6 and 9 cell surface expression on transplanted human hepatocytes and Huh7.5.1 cells. Cryopreserved primary human hepatocytes used for engraftment into upA-SCID mice were thawed and resuspended in PBS. Cell surface expression of CLDNs of human hepatocytes or Huh7.5.1 cells was performed in side-by-side experiments by flow cytometry using CLDN1, 6 and 9-specific rat mAb (OM-7D3-B3, WU-9E1-G2, YD-4E9-A2 respectively, 20 µg/mL) and PE-conjugated rat-specific secondary antibody (1:100) as described previously[3]. CLDN6 and 9-specific mAbs are described in[3].

Treatment of genotype 4 infected mice. Mice chronically infected (42 days post inoculation with serum) with HCV genotype 4 infectious serum (ED43[15]) received 500 µg CLDN1-specific mAb twice a week for 3 weeks followed by 200 µg twice a week up to the end of the study period. Blood was harvested by retro-orbital puncture under general anesthesia. Viral load and serum albumin was determined as described in Methods.

Immunohistochemistry of chimeric liver tissue. For human cytokeratin-18 (hCK18)-specific staining, livers of HCV-infected and CLDN1-specific or control mAb-treated mice were fixed in 4% paraformaldehyde, processed, embedded in paraffin prior to sectioning (10 microns) and stained as previously described[16]. For staining of human hepatocytes, tissue sections were incubated with 1:25-diluted anti-hCK18 mAb (M701029, clone DC10; Dako) overnight at 4°C. Following washing, stained cells were detected using the Vectastain Elite ABC kit (Vector Laboratories).

Liver function and biochemistry in human chimeric mice. Human albumin was quantified using ELISA (ref. E80-129, Bethyl Laboratories). The species-specificity of the assay was confirmed by the absence of detectable albumin in serum samples of non-transplanted uPA-SCID mice. Total bilirubin and transaminases (ALT, AST) activity were quantified by kinetic UV assay (Olympus Diagnostic).

Comparative analysis of antibody binding to human and mouse CLDN1. Primary human or mouse hepatocytes, Caco-2 cells or CLDN1-deficient 293T cells transfected with constructs pTrip-cerulean (pCTRL), pTrip-cerulean-human CLDN1 (pCLDN1 human) and pTrip-cerulean-mouse CLDN1 (pCLDN1 mouse) (all generous gifts from Dr. M. Evans, Mount Sinai School of Medicine, New York, NY[17]) were incubated with different concentrations of CLDN1-specific or control mAb for 1h as described[4]. Cellular binding of mAb was analyzed by subsequent incubation with a PE-labeled anti-rat secondary antibody (1:100, Jackson ImmunoResearch, 45 min, 4°C). Bound antibodies and transfection efficiency were analyzed as PE and cerulean mean fluorescence intensity (MFI) respectively using flow cytometry (LSR2, Becton Dickinson)[4].

Antibody biodistribution. Antibodies were labeled with Alexa-fluor 750 (RD-Biotech, Besançon, France). Eight week-old Balb/c mice were injected intraperitoneally with 500 µg of Alexa-fluor 750-labeled CLDN1-specific or control mAb. Organs were harvested 24 and 48h later as described[18] and *ex vivo* organ-specific fluorescence was detected with an IVIS Lumina 50 (Xenogen-Caliper-Perkin Elmer) and expressed as average efficiency.

Intestinal permeability assay. For *in vivo* intestinal permeability measurements, 7 week-old Balb/c mice (Janvier, Le Genest Saint Isle, France) were injected intraperitoneally with 250 µL PBS or CLDN1-specific or control mAb (2 mg/mL). Seven days later, the mice were given 130 µL of fluorescein-5.6-sulfonic acid[19] *per os* (10 mg/mL; Life Technologies) or 100 µL of 4 kDa or 40 kDa FITC-Dextran (22mg/mL; Sigma-Aldrich) suspended in carboxy-methyl cellulose 0.5% (W/V). Thirty minutes (FITC-sulfonic acid) or 3h (FITC-Dextran) later blood was collected and the fluorescence was determined on 10 µL of plasma diluted in 100 µL of PBS. Fluorescence was read on a fluorimeter (Berthold Mithras). Positive control mice received a 15 Gy dose of X-ray 3 days before the oral gavage. For *ex vivo* Ussing chamber experiments, the mice were treated as for *in vivo* assay except that mice were sacrificed at day 7. Specimens of jejunum and colon were collected in ice cold Hankôs Buffer Saline Solution (Life-Technologies). Specimens were detubulized and mounted in Ussing chambers (Physiological instruments, San Diego, CA, USA) (chamber surface of 0.0314 cm^2). Each chamber contained 2 mL of Hamôs Nutrient Mixture (HAM/F12, Life-Technologies). The media was continuously oxygenated by a gas flow of 95% O_2 and 5% CO_2 and maintained at 37°C. After an equilibration period of 30 min, 200 µL of apical medium was replaced by 200 µL of fluoresceinï 5.6 sulfonic acid (1 mg/mL). Every 30 min, the fluorescence level of basolateral aliquots of 150 µL was measured over a period of 180 min using a fluorimeter (Thermo SA). Paracellular permeability was determined by calculating the slope of the changes in fluorescence intensity over time using a linear regression fit model (GraphPad Software Company, La Jolla, CA, USA).

Total intestinal transit time. Seven week-old Balb/c mice randomly distributed by an animal technician were injected intraperitoneally with 250 µL PBS or CLDN1-specific or control mAb (2 mg/mL). Seven days later, mice were galvaged with carmine red solution (0.3 mg/g), a non-absorbable dye, suspended in carboxy-methyl cellulose 0.5% (W/V) as described[19]. Irradiated mice received a dose of 15 Gy X-ray (RS2000 biological irradiator, Rad Source, USA) 3 days before oral gavage. Total intestinal transit time was determined by the appearance of the first red fecal pellets after start of gavage.

***Ex vivo* intestinal conductance.** Specimens of jejunum and proximal colon were collected and treated as for *ex vivo* intestinal permeability assay. Ussing chambers were equipped with a pair of agar bridges connected to calomel half cells for measurement of transepithelial potential difference (PD). A pair of Agï AgCl disk electrodes was connected to a voltage clamp apparatus (Biomecatronics, Ruitz, France) that compensated for the solution resistance between the PD sensing bridges. Electrodes were juxtaposed between the Ussing chamber halves and the submucosal surface. Tissue conductance was calculated according to Ohmôs law.

***In vitro* trans-epithelial electrical resistance (TER) measurement.** TER was measured as described[20] with slight modifications. Briefly, Caco-2 cells were seeded on collagen-1 coated Transwell filters (Millipore, 0.4 µm pore size, 1.1 cm^2) and cultured in DMEM containing 10% FBS, non essential amino acids and penicillin (100 U/mL) streptomycin (100 µg/mL) for 20 days. Cells were apically treated with 100 µg/mL CLDN1-specific or control mAb or a combination of 500 ng/mL TNFŬ and IFNɔ at day 0 and TER was measured using Millicell ERS-2 (Millipore) at each time point. Cell surface CLDN1 expression of Caco2 cells was performed by flow cytometry

using CLDN1-specific mAb (OM-7D3-B3) as described above for human hepatocytes.

Biochemical and hematological parameters in Balb/c mice. Seven week-old Balb/c mice (Janvier, Le Genest Saint Isle, France) randomly distributed by an animal technician were injected intraperitoneally with 500 µg CLDN1-specific or control mAb. Serum biochemical parameters were determined 48h (ALT) and 7 days (ALT, AST, urea, creatinine, total proteins, albumin, total bilirubin, LDH, ALP) post-injection using an Olympus AU-400 automated laboratory work station (Olympus Diagnostic). A complete blood count including erythrocytes, leukocytes and platelets counts, hemoglobin and hematocrit measurement, differential leukocytes counts (neutrophils, basophils, eosinophils, lymphocytes, monocytes) and morphological analysis of blood cells was performed on an Advia 120 vet (Siemens). All analyses were performed blinded at the Institut Clinique de la Souris (ICS), Strasbourg, France.

Histopathology. Seven week-old Balb/c mice randomly distributed by an animal technician were intraperitoneally injected with 500 µg of CLDN1-specific or control mAb. One week later, mice were sacrificed and harvested organs were fixed in formaldehyde 4% (w/v) before paraffin embedding. Seven µm sections were obtained from paraffin blocks, stained with hematoxylin-eosin and submitted to histopathological analysis (blinded analysis by a pathologist at the Institut Clinique de la Souris (ICS), Strasbourg).

Tight junction functionality assay. Lentiviral shRNA libraries were obtained for human CLDN1 and human OCLN from Open Biosystems (Thermo Scientific, USA) and cloned into pLKO.1 vector. shRNA libraries were transfected into 293T cells to generate a lentiviral stock. HepG2 CD81 cells were transduced with the virus for 72h before selection of a stable population using puromycin (Sigma, UK). After stable knock down lines were generated, cells were cultured as per parental HepG2 CD81 cells. All experiments were carried out within 5 days of knock down to guarantee highest levels of gene suppression. Parental HepG2 CD81, CLDN1 shRNA HepG2 CD81 and OCLN shRNA HepG2 CD81 cells were seeded on glass coverslips at $4x10^4$cells/well and allowed to polarize for 5 days. All cells were fixed in 100% ice-cold methanol. Cells were permeabilized for 30 min in 0.05% saponin, 0.5% Bovine serum albumin (BSA) in phosphate buffered saline (PBS) and incubated with the following primary antibodies: anti-CLDN1 at 1:1000 (JAY.8 Invitrogen, mouse); anti-OCLN at 1:1000 (OC-3F10 Invitrogen, rabbit polyclonal) and anti-ZO-1 (Zymed, mouse) for 1h at room temperature in PBS-saponin-BSA. Cells were washed 3x in PBS-saponin-BSA before addition of a goat anti-mouse secondary Ab (Alexa 488, Invitrogen) at a 1:1000 dilution in PBS-saponin-BSA or a goat anti-rabbit secondary Ab (Alexa 488; Invitrogen) for 1h at RT. Cells were washed 3 x in PBS-saponin-BSA before counter-staining with 4',6-diamidino-2-phenylindole (DAPI, Invitrogen) in PBS for 5 min. Coverslips were mounted on glass slides (ProLong Gold antifade, Invitrogen). Laser scanning confocal microscopy (LSCM) was performed on a Zeiss Meta Head Confocal Microscope with a 63x water immersion objective. To determine the functionality of TJs HepG2 CD81, CLDN1 shRNA HepG2 CD81 and OCLN shRNA HepG2 CD81 cells were incubated with 5mM 5-chloromethylfluorescein diacetate (CMFDA; Invitrogen) at 37^{o}C for 10 min to allow translocation to bile-canalicular (BC) lumen. After washing extensively with PBS, the capacity of BC to retain CMFDA was enumerated using a fluorescence microscope. TJ integrity was

determined by quantifying the number BC which retained CMFDA in 10 fields of view on 3 replicate coverslips. Restrictions of CMFDA to the BC indicate that polarized HepG2 cells have functional TJs. To determine the effect of antibodies on TJ integrity, HepG2 CD81 cells were incubated, as described above, in presence of 10 µg/mL of CD81-specific (2s131), SR-BI-specific (P72) or CLDN1-specific (OM-7D3-B3) mAbs for 1h at 37°C. During the hour incubation, TJ integrity was determined (as described above) by quantifying the number BC which retained CMFDA in 10 fields of view on 3 replicate coverslips at 15 min intervals.

CLDN1 internalization assay. Huh7.5.1 cells were incubated at 4 or 37°C for 1h with control or CLDN1-specific mAb (20 µg/mL), washed twice in ice-cold PBS, fixed for 10 min in 4% PFA, washed twice with ice-cold PBS and incubated for 45 min with PE-labeled anti-rat secondary antibody (1:100, Jackson ImmunoResearch). Bound antibodies were analyzed using flow cytometry (LSR2, Becton Dickinson).

Receptor association using Förster resonance energy transfer (FRET). Homotypic and heterotypic interaction of CD81 and CLDN1 were analyzed in 293T cells transduced to express AcGFP and DsRed tagged CD81 and CLDN1 as described[21]. Transfected 293-T cells were seeded on 22 mm diameter borosilicate glass coverslips in absence or in presence of CLDN1-specific mAb (10 µg/mL) and imaged using a Zeiss MetaHead confocal system. The samples were photobleached at 561 nm to prevent the energy transfer from the AcGFP fluorophore to DsRED fluorophore with images being taken before and after the photobleach. The data from 10 independent experiments were normalized to calculate the localized expression.

Cell-cell transmission of HCV. Cell-cell transmission of HCV was assessed as described[5]. Briefly, producer Huh7.5.1 cells were electroporated with HCV Jc1 RNA and co-cultured with naïve target Huh7.5-GFP cells in the presence or absence of an anti-HCV positive serum from a chronically infected patient (1:50 dilution), HCV E1-neutralizing antibody (mouse IGH433, 100 µg/mL), HCV E2-neutralizing antibody (mouse AP33, 100 µg/mL), CLDN1-specific (rat clone OM-7D3-B3, 10 µg/mL), SR-BI-specific (mouse clone NK-8H5-E3, 10 µg/mL) mAb or corresponding isotype control (10 µg/mL). AP33 (25 µg/mL) was added to block cell-free transmission[5]. After 24h of co-culture, cells were fixed with PFA, stained with either a mouse NS5A-specific antibody (0.1 µg/mL, Virostat) or a human anti-E2 antibody (clone CHB-23, 8.8 µg/mL). Infected cells were revealed by a PE-labelled secondary antibody and analyzed by flow cytometry[5]. Total and cell-cell transmission were defined as percentage HCV infection of Huh7.5-GFP+ target cells (Ti) in the absence (total transmission) or presence (cell-cell transmission) of AP33 as described[5]. To assess the inhibition of viral spread, CLDN1-specific or control mAb (0.1, 1, 10, 100 µg/mL) were added 48h after infection of Huh7.5.1 cells with HCVcc Luc-Jc1 reporter virus[22]. Medium containing CLDN1-specifc or control mAb was replenished every second day. HCV replication was quantified by luciferase reporter expression at indicated time points.

Effect of CLDN1-specific mAb on replication and assembly and release. Huh7.5 shCD81.1 cells were electroporated with 10 µg *in vitro* transcripts of JcR2a as described[12]. Electroporated cells were resuspended in DMEM and seeded into 24-well plates. Eight hours later, medium was replaced by the diluted CLDN1-specific or control mAb (100 µg/mL). After 24, 48, 72 and 96h (triplicates for each time point),

supernatants were harvested and clarified by filtration using a 0.45 µM pore filter and cells were lysed with 0.5% Triton X-100. Clarified supernatants and cell lysates were used to measure HCV core protein amounts by using a diagnostic luminescence assay (6L47, ARCHITECT HCV Ag Reagent Kit, Abbott Diagnostics, Abbott Park, USA) according to the manufacturer's instructions. To determine amounts of infectious HCV contained in the supernatants, we used a limiting dilution assay and Huh7.5 cells as described elsewhere[12]. In brief, Huh7.5 cells were seeded into 24-well plates at a density of $4x10^4$ cells per well. One day post seeding, 500 µl of a given supernatant was added to the cells (duplicates). In some cases, supernatants of CLDN1- or control mAb-treated cells were mixed with the same volume of JcR2a-containing supernatant. In all cases, cells were harvested for Renilla luciferase assay 72h after inoculation.

Small RNA library preparation. Libraries were prepared as previously described[23] with some modifications. Briefly, total RNA was extracted from 10 day mock-infected and HCV-infected Huh7.5.1 cells, after 24h treatment with CLDN1-specific or control mAb, using TRI-Reagent (Ambion). 10 µg of total RNA were size fractionated on a 17.5% urea denaturing polyacrylamide gel. The 19-24 nt band was excised, crushed and solved in 2 volumes of 0.3 M NaCl by overnight agitation at 4°C. Small RNAs were sequentially ligated to 3ôadapter (5ôP-NNNNTGGAATTCTCGGGTGCCAAGG-[C7amino]) and then to 5ô adapter (GUUCAGAGUUCUACAGUCCACGAUCNNNN) (with T4 RNA Ligase 2 and T4 RNA Ligase 1, respectively). Four degenerate bases were respectively included at the 3ôend of the 5ôadapter and at the 5ôend of the 3ô adapter to minimize ligation bias due to secondary structure formation[24,25]. After each ligation step, the product was purified on denaturing polyacrylamide gel. In order to generate cDNA libraries, RNA was reverse transcribed with SuperScript III RT (Invitrogen), then amplified by PCR with a common forward primer and different reverse primers for multiplex sequencing. PCR products were sent for large-scale sequencing, which was performed by the IGBMC Microarray and Sequencing platform, member of the France Genomique program, using an Illumina HiSeq 2500 instrument with a read length of 50 nt.

Bioinformatic analysis of deep sequencing data. Sequencing reads were preprocessed and annotated using a set of custom Python scripts pipelining different tools. The Dustmasker program[26] and FASTX-Toolkit (http://hannonlab.cshl.edu/fastx_toolkit) were first applied to filter out low complexity reads and remove instances of the 3ôadapter. Degenerate bases incorporated during the library preparation protocol were also trimmed at this step. Remaining reads of 15 to 32 nt in length were then mapped simultaneously to the human (assembly version hg19 ï UCSC repository) and HCV (reconstructed from GenBank sequences AF177036.1 and AB047639.1) genomes, using Bowtie 0.12.7[27]. Up to 2 mismatches in total with no more than 1 mismatch in the first 15 nucleotides of each read were permitted. In addition, only alignments from the lowest mismatch-stratum were recorded and reads that could map to more than 50 loci were discarded. Human miRNAs (miRBase Release 19[28]) were annotated in each library using BEDTools 2.16.2[29] by comparing their genomic coordinates to those of the aligned reads, and by keeping reads with at least 80% of their length inside the genomic features. During the quantification process, multiple mapped reads were weighted by the number of mapping sites in miRNAs. To allow subsequent comparative expression analysis, miRNA measures were normalized per million miRNA reads (RPMmi, Reads Per

Million miRNA reads), and only miRNAs present in at least one of the libraries with a minimum of 10 RPMmi were kept for further analysis. Hierarchical clustering with complete linkage and euclidean distance was performed using the union of the 100 most abundant miRNAs in each library and Log2 transformed data.

Inhibition of HCV infection by protein kinase inhibitors. Huh7.5.1. cells were seeded into 96 well-plates ($2x10^3$ cells/well) in triplicates and infected 24 h later for 3 days with HCVcc Luc-Jc1. Medium was then removed and replaced with medium containing increasing concentrations (0.01, 0.1, 0.5, 1, 5, 10, 50 and 100 µM) of erlotinib (LC Laboratories) or UO126 (Calbiochem) and final concentration of 1% DMSO. Control medium contained 1% DMSO. Three days later, cell viability was assessed by PrestoBlue (Invitrogen) as recommended by the manufacturer and determined at 535 nm. HCV replication was quantified by luciferase activity measurement on cell lysates.

Mathematical model of viral load decline. The standard mathematical model of viral infection by Neumann *et al*.[6] was used to analyze viral decline after mAb treatment. In brief, this differential equations model is based on mass action kinetics, and contains the three species uninfected (target) cells T, infected cells I and virus particles V. Uninfected cells T are produced with rate s and die with rate d. Furthermore, uninfected cells become infected with virus V with rate **ß**V. Infected cells I die with rate **ŭ**, and produce virus V at rate **ɟ** . Finally virus particles are cleared with rate c. The effect of the CLDN1-specific mAb is assumed to reduce the infection rate **ß** by a factor (1-**ɖ**). Assuming that the infection is at a steady state before treatment and that the uninfected cells T are not limiting (dT/dt=0), the system of equations can be solved analytically. We implemented the model in Matlab (The Mathworks) and fitted model parameters to the experimental data, minimizing the sum of squared errors between model prediction and data points.

Detection of HCV-induced apoptosis in Huh7.5.1 cells. Chronic HCV infection was established by electroporation of HCV RNA (Jc1) into Huh7.5.1 as described[8]. To analyze apoptosis via caspase activity or membrane changes one week after establishment of the infection, cells were labeled the using CellEvent Caspase-3/7 Green detection kit (Life Technologies) for detection of activated caspase-3/7 or using a labeled annexin V conjugate (Roche) for studying the externalization of phosphatidylserine according to the manufacturersôinstructions. Labeled cells were analyzed using a MACSQuant Analyzer (Miltenyl Biotec). Mock-electroporated cells were analyzed in parallel and served as negative control.

Kinetics of viral infection and number of infected cells in persistently infected Huh7.5.1 cells. Persistent HCV infection was established by electroporation of HCV RNA (Jc1) into Huh7.5.1 cells cultured in medium containing 1% DMSO as described[8]. One week after electroporation, cells were continuously incubated with 100 µg/mL control or CLDN1-specific mAb. Cell culture medium containing antibody was replenished every 3 to 4 days. The percentage of HCV-infected cells was determined by flow cytometry of permeabilized cells harvested at different time points and stained with an HCV E2-specific mAb (AP33) followed by a PE-conjugated anti-mouse IgG (BD Bioscience) as described[8]. Analyses were performed on a MACSQuant Analyzer. HCV RNA (viral load) was quantified by RT-PCR[7] and absent

HCV RNA was confirmed using the clinically approved Abbott Real Time HCV assay (sensitivity 120 IU HCV RNA/sample).

SUPPLEMENTARY REFERENCES

1. Karpati, G., Carpenter, S. & Wolfe, L.S. Clinical and experimental studies on lipofuscin in skeletal muscle fibers. *Lipofuscin. Nagy, Z. (ed) State of the Art. Elsevier, Amsterdam*, 195-215 (1988).
2. Moriya, K.*, et al.* Oxidative stress in the absence of inflammation in a mouse model for hepatitis C virus-associated hepatocarcinogenesis. *Cancer Res* **61**, 4365-4370 (2001).
3. Fofana, I.*, et al.* Functional analysis of claudin-6 and claudin-9 as entry factors for hepatitis C virus infection of human hepatocytes by using monoclonal antibodies. *J Virol* **87**, 10405-10410 (2013).
4. Fofana, I.*, et al.* Monoclonal anti-claudin 1 antibodies prevent hepatitis C virus infection of primary human hepatocytes. *Gastroenterology* **139**, 953-964.e954 (2010).
5. Lupberger, J.*, et al.* EGFR and EphA2 are host factors for hepatitis C virus entry and possible targets for antiviral therapy. *Nat Med* **17**, 589-595 (2011).
6. Neumann, A.U.*, et al.* Hepatitis C viral dynamics in vivo and the antiviral efficacy of interferon-alpha therapy. *Science* **282**, 103-107 (1998).
7. Pietschmann, T.*, et al.* Production of infectious genotype 1b virus particles in cell culture and impairment by replication enhancing mutations. *PLoS Pathog* **5**, e1000475 (2009).
8. Xiao, F.*, et al.* Hepatitis C virus cell-cell transmission and resistance to direct-acting antiviral agents. *PLoS Pathog* **10**, e1004128 (2014).
9. Fafi-Kremer, S.*, et al.* Viral entry and escape from antibody-mediated neutralization influence hepatitis C virus reinfection in liver transplantation. *J Exp Med* **207**, 2019-2031 (2010).
10. Pestka, J.M.*, et al.* Rapid induction of virus-neutralizing antibodies and viral clearance in a single-source outbreak of hepatitis C. *Proc Natl Acad Sci U S A* **104**, 6025-6030 (2007).
11. Reiss, S.*, et al.* Recruitment and activation of a lipid kinase by hepatitis C virus NS5A is essential for integrity of the membranous replication compartment. *Cell Host Microbe* **9**, 32-45 (2011).
12. Kaul, A., Woerz, I., Meuleman, P., Leroux-Roels, G. & Bartenschlager, R. Cell culture adaptation of hepatitis C virus and in vivo viability of an adapted variant. *J Virol* **81**, 13168-13179 (2007).
13. Zhong, J.*, et al.* Robust hepatitis C virus infection in vitro. *Proc Natl Acad Sci U S A* **102**, 9294-9299 (2005).
14. Da Costa, D.*, et al.* Reconstitution of the entire hepatitis C virus life cycle in non-hepatic cells. *J Virol* **86**, 11919-11925 (2012).
15. Bukh, J.*, et al.* Challenge pools of hepatitis C virus genotypes 1-6 prototype strains: replication fitness and pathogenicity in chimpanzees and human liver-chimeric mouse models. *J Infect Dis* **201**, 1381-1389 (2010).
16. Mercer, D.F.*, et al.* Hepatitis C virus replication in mice with chimeric human livers. *Nat Med* **7**, 927-933 (2001).
17. Evans, M.J.*, et al.* Claudin-1 is a hepatitis C virus co-receptor required for a late step in entry. *Nature* **446**, 801-805 (2007).
18. Leboeuf, C.*, et al.* In vivo proof of concept of adoptive immunotherapy for hepatocellular carcinoma using allogeneic suicide gene-modified killer cells. *Mol Ther* **22**, 634-644 (2014).

19. Tasselli, M.*, et al.* Effects of oral administration of rotenone on gastrointestinal functions in mice. *Neurogastroenterol Motil* **25**, e183-193 (2013).
20. Piche, T.*, et al.* Impaired intestinal barrier integrity in the colon of patients with irritable bowel syndrome: involvement of soluble mediators. *Gut* **58**, 196-201 (2009).
21. Harris, H.J.*, et al.* Claudin association with CD81 defines hepatitis C virus entry. *J Biol Chem* **285**, 21092-21102 (2010).
22. Koutsoudakis, G.*, et al.* Characterization of the early steps of hepatitis C virus infection by using luciferase reporter viruses. *J Virol* **80**, 5308-5320 (2006).
23. Pfeffer, S. Identification of virally encoded microRNAs. *Methods Enzymol* **427**, 51-63 (2007).
24. Sorefan, K.*, et al.* Reducing ligation bias of small RNAs in libraries for next generation sequencing. *Silence* **3**, 4 (2012).
25. Hafner, M.*, et al.* RNA-ligase-dependent biases in miRNA representation in deep-sequenced small RNA cDNA libraries. *RNA* **17**, 1697-1712 (2011).
26. Morgulis, A., Gertz, E.M., Schaffer, A.A. & Agarwala, R. A fast and symmetric DUST implementation to mask low-complexity DNA sequences. *J Comput Biol* **13**, 1028-1040 (2006).
27. Langmead, B., Trapnell, C., Pop, M. & Salzberg, S.L. Ultrafast and memory-efficient alignment of short DNA sequences to the human genome. *Genome Biol* **10**, R25 (2009).
28. Griffiths-Jones, S. The microRNA Registry. *Nucleic Acids Res* **32**, D109-111 (2004).
29. Quinlan, A.R. & Hall, I.M. BEDTools: a flexible suite of utilities for comparing genomic features. *Bioinformatics* **26**, 841-842 (2010).